Brain, Behavior, & Immunity - Health 23 (2022) 100458

Contents lists available at ScienceDirect

Brain, Behavior, & Immunity - Health

journal homepage: www.editorialmanager.com/bbih/default.aspx

Prenatal administration of multipotent adult progenitor cells modulates the systemic and cerebral immune response in an ovine model of chorioamnionitis

Luise Klein [a,b,c], Daan R.M.G. Ophelders [a,b], Daniel van den Hove [c,d,e], Maurits Damoiseaux [a,b], Bart P.F. Rutten [c,e], Chris P.M. Reutelingsperger [f], Leon J. Schurgers [f], Tim G.A.M. Wolfs [a,b,*]

[a] School for Oncology and Reproduction (GROW), Maastricht University, Maastricht, the Netherlands
[b] Department of Pediatrics, Maastricht University, Maastricht, the Netherlands
[c] School for Mental Health and Neuroscience (MHeNs), Maastricht University, Maastricht, the Netherlands
[d] Department of Psychiatry, Psychosomatics and Psychotherapy, University of Würzburg, Würzburg, Germany
[e] Department of Psychiatry and Neuropsychology, European Graduate School of Neuroscience (EURON), Faculty of Health, Medicine and Life Sciences (FHML), Maastricht University, Maastricht, the Netherlands
[f] Department of Biochemistry, Cardiovascular Research Institute Maastricht, Maastricht University, the Netherlands

ARTICLE INFO

Keywords:
Antenatal inflammation
Stem cell therapy
Immunomodulation
Neuro-immune axis

ABSTRACT

Systemic and cerebral inflammation following antenatal infection (e.g. chorioamnionitis) and dysregulation of the blood brain barrier (BBB) are major risk factors for abnormal neonatal brain development. Administration of multipotent adult progenitor cells (MAPCs) represents an interesting pharmacological strategy as modulator of the peripheral and cerebral immune response and protector of BBB integrity. We studied the immunomodulatory and protective cerebrovascular potential of prenatally administered MAPCs in a preclinical ovine model for antenatal inflammation.

Ovine fetuses were intra-amniotically (i.a.) exposed to lipopolysaccharide (LPS) or saline at gestational day 125, followed by the intravenous administration of $1*10^7$ MAPCs or saline at gestational day 127. Circulating inflammation markers were measured. Fetal brains were examined immuno-histochemically post-mortem at gestational day 132.

Fetal plasma IL-6 levels were elevated significantly 24 h after LPS administration. *In utero* systemic MAPC treatment after LPS exposure increased Annexin A1 (ANXA1) expression in the cerebrovascular endothelium, indicating enforcement of BBB integrity, and increased the number of leukocytes at brain barriers throughout the brain. Further characterisation of brain barrier-associated leukocytes showed that monocyte/choroid plexus macrophage (IBA-1^+/CD206^+) and neutrophil (MPO^+) populations predominantly contributed to the LPS-MAPC-induced increase of CD45^+cells. In the choroid plexus, the percentage of leukocytes expressing the proresolving mediator ANXA1 tended to be decreased after LPS-induced antenatal inflammation, an effect reversed by systemic MAPC treatment. Accordingly, expression levels of ANXA1 per leukocyte were decreased after LPS and restored after subsequent MAPC treatment.

Increased expression of ANXA1 by the cerebrovasculature and immune cells at brain barriers following MAPC treatment in an infectious setting indicate a MAPC driven early defence mechanism to protect the neonatal brain against infection-driven inflammation and potential additional pro-inflammatory insults in the neonatal period.

1. Introduction

Worldwide, 15 million babies are born preterm (<37 weeks of gestation) per year (Blencowe et al., 2012). Antenatal infection, also referred to as chorioamnionitis, is an important risk factor for preterm birth and is associated with inflammation driven neurodevelopmental

* Corresponding author. School for Oncology and Reproduction (GROW), Maastricht University, Maastricht, the Netherlands.
E-mail addresses: l.klein@maastrichtuniversity.nl (L. Klein), d.ophelders@maastrichtuniversity.nl (D.R.M.G. Ophelders), d.vandenhove@maastrichtuniversity.nl (D. van den Hove), maurits.damoiseaux@student.maastrichtuniversity.nl (M. Damoiseaux), b.rutten@maastrichtuniversity.nl (B.P.F. Rutten), c.reutelingsperger@maastrichtuniversity.nl (C.P.M. Reutelingsperger), l.schurgers@maastrichtuniversity.nl (L.J. Schurgers), tim.wolfs@maastrichtuniversity.nl (T.G.A.M. Wolfs).

https://doi.org/10.1016/j.bbih.2022.100458
Received 11 January 2022; Received in revised form 17 March 2022; Accepted 31 March 2022
Available online 2 May 2022

disorders and consecutive life-long disabilities (Rand et al., 2016; Wu and Colford, 2000). Exposure of the fetus to harmful microorganisms and/or inflammatory agents can result in fetal inflammatory response syndrome (FIRS), clinically characterized by an acute increase in pro-inflammatory cytokine levels in the fetal plasma and changes in the fetal hematological profile (e.g. leucocytosis) (Gussenhoven et al., 2018; Helmo et al., 2018; Mestan et al., 2009; Romero et al., 2011; Yap and Perlman, 2020). The mechanisms underlying injury of the immature brain upon intra-amniotic (i.a.) infections are still incompletely understood. *In vitro* and *in vivo* evidence demonstrates that pro-inflammatory cytokines, elevated in FIRS, can induce a permeable blood brain barrier (BBB), thereby facilitating entry of peripheral immune cells contributing to neuroinflammation (Yan et al., 2004; Smyth et al., 2018; Banks et al., 2015; Stolp et al., 2005; Moretti et al., 2015). Pro-inflammatory cytokines activate vascular endothelial cells, which secrete pro-inflammatory mediators such as prostaglandins at the basal side reaching the brain parenchyma, further destabilizing BBB integrity and activation of the resident immune cells of the brain (Yan et al., 2004; Choi et al., 2009; Hagberg et al., 2015; Paton et al., 2017; Yawno et al., 2013, 2017).

Several barriers near the brain protect the normally immune-privileged central nervous system (CNS) and constitute possible entry routes/neuroimmune cross-talk points for the peripheral immune system during neuroinflammation. These interfaces include 1) the blood-brain barrier (BBB) in the brain parenchyma; 2) the blood-cerebrospinal fluid-barrier (BCSFB), i.e. choroid plexus; and 3) the meningeal barrier consisting out of three more barriers including the blood-leptomeningeal barrier (BLMB) (Saunders et al., 2019). Schwartz and colleagues proposed that brain barriers, especially the choroid plexus, act as educational gate for entry of peripheral immune cells to the CNS (Shechter et al., 2013a, 2013b; Schwartz and Baruch, 2014). In a model for neonatal systemic inflammation, peripheral immune cells, particularly monocytes and neutrophils, were shown to accumulate in the choroid plexus, indicating a role for cerebral recruitment of peripheral immune cells via the choroid plexus (Mottahedin et al., 2017, 2019).

Absence of treatment strategies for preterm brain injury after antenatal infection/inflammation (Yap and Perlman, 2020; Paton et al., 2017) stresses the need for novel therapeutic interventions that can be safely applied. Mesenchymal stromal cells (MSCs) including multipotent adult progenitor cells (MAPCs) have been shown to modulate the cerebral and peripheral immune response and maintain or restore BBB integrity. Accordingly these stem cells have been successfully used to improve outcomes of the CNS in either neonatal or adult injury (Yawno et al., 2013; Yawno et al., 2017; B ö rger et al., 2017; Doeppner et al., 2015; Nair et al., 2020; Vaes et al., 2019; Drommelschmidt et al., 2017; Walker et al., 2010; Walker et al., 2012).

Exogenous stem cells are considered to exert their effects at least in part via their secretome. Annexin A1 (ANXA1), as essential molecule in the innate anti-inflammatory immune response is an interesting candidate in this context (Perretti and D'Acquisto, 2009; McArthur et al., 2010). In the CNS, it acts in a neuroprotective way by maintaining BBB integrity and inducing an anti-inflammatory phenotype in microglia with enhanced phagocytic capacity (Perretti and D'Acquisto, 2009; McArthur et al., 2010; Cristante et al., 2013; Park et al., 2017; Hu et al., 2016; Loiola et al., 2019). This multifunctional molecule has been shown to act on diminishing inflammation in the periphery as well by skewing macrophages towards a restorative phenotype (Ferraro et al., 2019; Locatelli et al., 2014; McArthur et al., 2020). Macrophages can be directed towards an anti-inflammatory phenotype through an interplay with migrating neutrophils. The neutrophil is considered to be the main source of endogenous ANXA1 carried into inflamed tissues (McArthur et al., 2020; Prame Kumar et al., 2018; Sugimoto et al., 2016). Additionally, ANXA1 was identified as key player for regenerative effects of stem cell therapy in pancreatic, hepatic and pulmonary pathologies (Zagoura et al., 2019; Rackham et al., 2016; Tovar et al., 2020). Together, this highlights ANXA1 as important effector molecule of immunomodulatory therapy.

Immunomodulatory, and neuro-protective properties of MAPCs, e.g. those linked to BBB integrity, have raised increasing interest in the therapeutic potential of MAPCs in inflammation-induced brain injury (Walker et al., 2010, 2012). We hypothesized that in a model of LPS-induced chorioamnionitis, early administration of MAPCs could modulate the peripheral and cerebral inflammatory response and protect the cerebrovasculature. To test this hypothesis, we studied the effect of i.a. LPS exposure and i.v. MAPC administration on phenotypic characteristics of immune cells at the BBB and brain parenchyma and the expression of the BBB integrity marker ANXA1.

2. Methods & materials

2.1. Study approval

Experimental procedures and the study design were approved by the Central Authority for Scientific Procedures on Animals (CCD), conducted in accordance with ARRIVE guidelines and in line with institutional guidelines for animal experiments of the Animal Welfare Body of Maastricht University, the Netherlands.

2.2. Experimental design and animals

27 Texel ewes were randomized into four groups: (1) i.a. saline and intravenous (i.v.) saline treatment (SAL-SAL, n = 7, (2) i.a. 5 mg lipopolysaccharide (LPS, O55:B5; L2880, Sigma-Aldrich, Zwijndrecht, NL; 5 mg) and i.v. saline treatment (LPS-SAL, n = 7), (3) i.a. saline and i.v. MAPC treatment (SAL-MAPC, n = 7), and (4) i.a. LPS and i.v. MAPC treatment (LPS-MAPC, n = 6) (Fig. 1). On gestational age (GA) 131 or GA 132, four ewes spontaneously aborted (SAL-MAPC n = 2, LPS-SAL n = 2), which was an exclusion criterion. In the SAL-SAL group two accidental twins were included, resulting in the following number of fetuses per treatment group: SAL-SAL n = 9, SAL-MAPC n = 5, LPS-SAL n = 5, LPS-MAPC n = 6.

2.3. Surgery and monitoring

Fetuses of time-mated Texel ewes were instrumented at 121 days of GA as previously described with slight modifications in the protocol (Jellema et al., 2013; Nikiforou et al., 2015). 121 GA in sheep (full term is approximately 147 days) is comparable to 32–33 weeks of human gestation, corresponding to moderate/late preterm babies, with regard to brain development (Back et al., 2012). Ewes were anesthetized by induction of thiopental (15 mg/kg) i.v.. During surgery, general anesthesia was maintained by 1%–2% isoflurane and in combination with remifentanyl (0.75 μg kg^{-1} min^{-1}) i.v. for analgesia. A catheter was introduced into the maternal saphenous vein to obtain blood samples and administer prophylactic antibiotics (amoxicillin clavulanic acid) during 4 days of recovery after surgery. Fetuses were exposed by median laparotomy and hysterotomy, and two 3.5 French umbilical vessel catheters (Covidien, Mansfield, MA) were placed in the femoral artery and vein for blood pressure recordings, blood sampling, and administration of stem cells. An additional catheter was placed in the amniotic sac for recordings of amniotic pressure and administration of LPS. All leads were exteriorized through a trocar hole in the maternal flank of the ewe and were continuously flushed (except from the amniotic catheter) with heparinized saline (25 IU/mL). Postoperatively, animals were housed in confined space with access to food and water ad libitum. Fetal blood was taken every morning before any other administration (i.a. LPS/SAL or i.v. MAPC/SAL) was performed to monitor the fetal systemic immune response after i.a. LPS administration at 125 days of gestation and i.v. administration of $1*10^7$ bone marrow derived MAPCs (ReGenesys BVBA, Heverlee, BE) at day 127 GA. At day 132 of gestation, all fetuses were surgically delivered by C-section and immediately

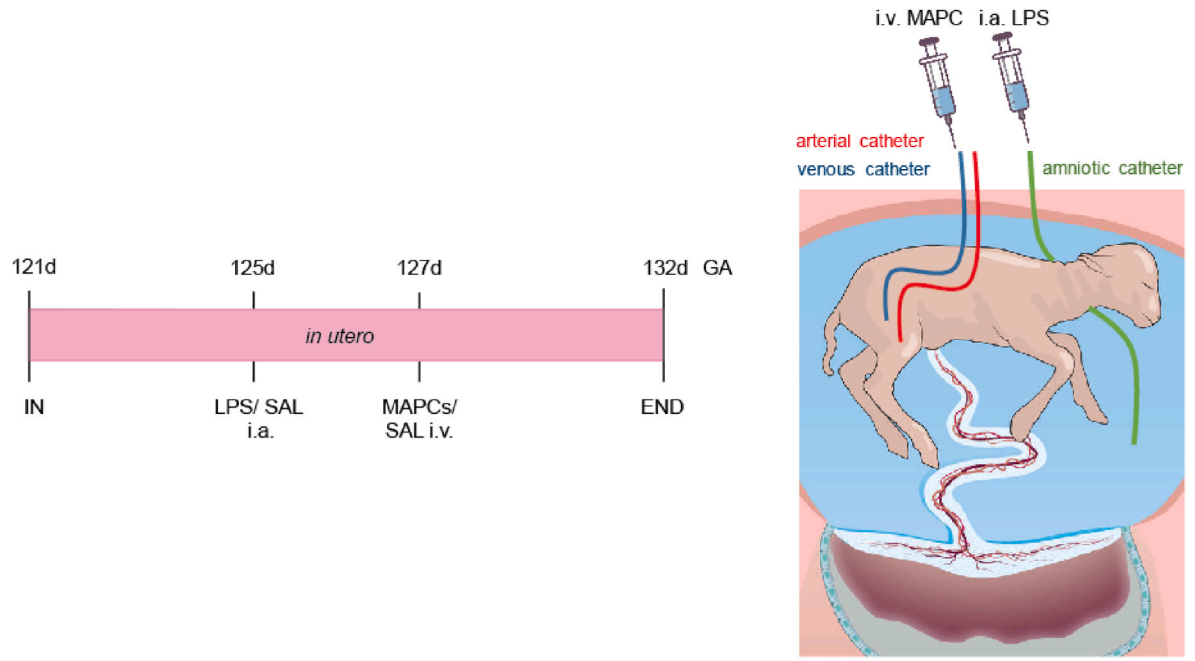

Fig. 1. Experimental design. Pregnant ewes were instrumented at day 121 of gestation to receive an i.a. injection of LPS/SAL at day 125 of GA and an i.v. injection of MAPC/SAL at day 127 of GA. Fetuses were delivered at day 132 of GA. Abbreviations: d; day, i.a.; intra-amniotic, i.v.; intravenous, IN; instrumentation, LPS; lipopolysaccharide, SAL; saline, MAPC; multipotent adult progenitor cells, GA; gestational age.

euthanized with i.v. injected pentobarbitone (100 mg/kg). Fetal brains were removed from the skull for further processing. Before fixation 4% paraformaldehyde in 0.1 M phosphate buffer (pH 7.4), the choroid plexus was removed and cryopreserved in liquid nitrogen-cooled isopentane for cryosectioning.

2.4. Multipotent adult progenitor cells

Cells were isolated and expanded on the Quantum Cell Expansion System (Terumo BCT, Lakewood, CO) as described (Cunha et al., 2017) in off-the-shelf xenobiotic free media supplemented with additional MAPC growth components, maintained under low oxygen tension, and stored in liquid nitrogen gas phase until use. Cells were phenotyped in terms of marker expression and differentiation potential, as described (Crabb é et al., 2016). In short, MAPCs were phenotyped by their ability to differentiate into adipocytes, chondrocytes and osteoblasts, flow cytometry ($CD13^+$, $CD90^+$, CD105+, CD45-, HLAII-, CD34-), expression of key MAPC markers miR-204-5p, miR-20a-5p, miR-18a-5p, miR-106a-5p, miR-17-5p, and miR-155-5p and no expression for seven key MSC miRNAs (miR-335-5p, miR-145-5p, miR-143-3p, miR-27b-3p, miR-125b-5p, miR-26a-5p, miR-152-3p). Proangiogenic activity was measured by tube formation on human umbilical vein endothelial cells and immunosuppressive capacity by their ability to reduce the proliferation of human, third party CD3/28 activated T-cells. MAPCs (1×10^7 cells/mL) were thawed at room temperature for maximally 1 h and sterile administered in a single 1 mL bolus via the femoral vein to the fetuses (127 GA) randomized to MAPC treatment.

2.5. Enzyme-linked immunosorbent assay for IL-6 in fetal circulation

Levels of IL-6 were measured in fetal plasma as markers for systemic inflammation using ovine-specific sandwich enzyme-linked immunosorbent assays (ELISA) as described in more detail previously (Gussenhoven et al., 2017, 2018). Concentrations were expressed relative to the standard curve. Values falling below the detection limit (39 pg/mL) were given an arbitrary value of 1 and values above the threshold (625 pg/mL) were assigned as 1250 pg/mL to allow statistical analysis.

2.6. Immunohistochemistry – brain regions, type of sample and markers

Immunohistochemical analysis was performed with cryosections of the choroid plexus (BCSFB) and paraffin-embedded tissue of the right hemisphere of each animal. To analyze the BBB and BLMB, paraffin sections of the frontal motor cortex, striatum, and hippocampus/midthalamus (Fig. 2) were used.

Table 1 lists molecular markers used to characterize the cerebrovasculature (BBB, BLMB, BCSFB) and circulating immune cells.

2.6.1. Immunohistochemistry of cryosections

The frozen choroid plexus (BCSFB) was embedded in O.C.T. embedding matrix (CellPath, Newtown, UK) and slides (7 μm) were cut using a Leica CM3050 S cryostat (Leica Biosystems Nussloch GmbH, Nuβloch, DE). Cryosections were dried for 15 min at 37 °C and fixated in ice-cold methanol for 15 min. CD45, ANXA1 co-staining and MPO staining was performed in tris-buffered saline (TBS) containing 0.1% Triton X-100. CD206, ANXA1 co-staining was conducted in TBS with 0.02% Tween20. Endogenous peroxidase activity was inactivated by incubation in 0.3% H_2O_2 diluted in the appropriate staining buffer for 20 min. Non-specific binding was prevented by incubation with 4% normal goat serum. Tissues were incubated with the primary antibodies for CD45 (1:1000, monoclonal mouse IgG1 anti-sheep CD45, MCA2220GA, Bio-Rad, Hercules, CA), CD206 (1:1000, monoclonal mouse IgG1 anti-CD206, DDX0380P05, Novus Biologicals, Oxon, UK), ANXA1 (1:300, polyclonal rabbit anti-ANXA1, ab137745, Abcam, Cambridge, UK) and MPO (1:200, polyclonal rabbit anti-human MPO, A0398, DAKO Agilent Technologies, Santa Clara, CA) in a humidified box at 4 °C overnight, followed by incubation with the appropriate secondary antibody at 1:200 (polyclonal goat anti-mouse, Alexa Fluor 594 or polyclonal donkey anti-rabbit, Alexa Fluor 488, Thermo Fisher Scientific, Waltham, MA) for 1 h. Nuclei were stained by incubating the tissue with 4',6-diamidino-2-fenylindool (DAPI, 0.5 μg/mL) for 5 min in the dark at room temperature. Lastly, slides were mounted with fluorescent mounting medium (Faramount mounting medium, Agilent DAKO, Amstelveen, NL).

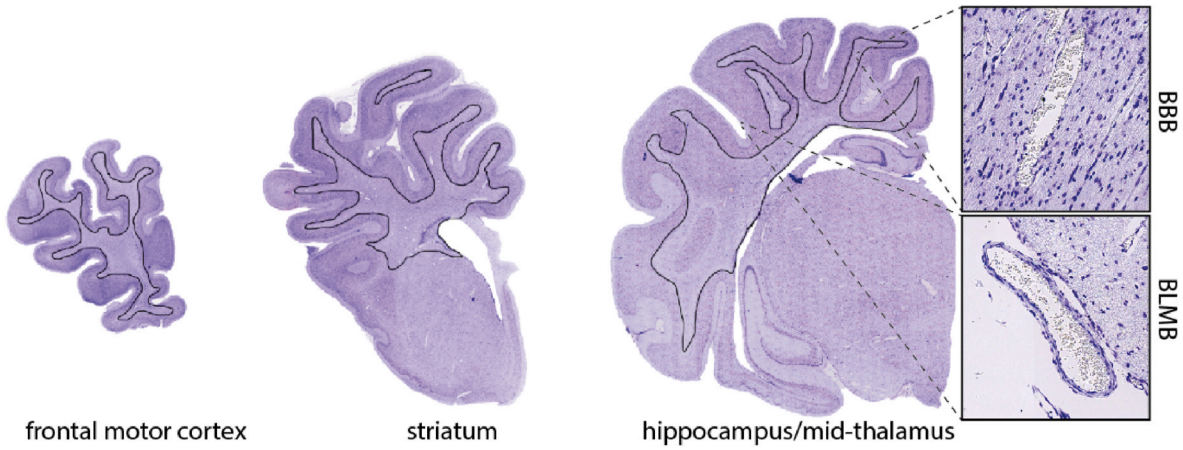

Fig. 2. Brain regions and barriers of interest analysed by immunohistochemistry. Nissl staining of the selected regions of interest for immunohistochemical staining of the paraffin-embedded coronal brain sections. Coronal section at the plane of 1) the frontal motor cortex and beginning of the lateral ventricle, 2) the striatum, and 3) the hippocampus/mid-thalamus. In all three regions of interest, blood vessels of the blood-brain barrier (BBB) were selected in the encircled areas and blood vessels of the blood leptomeningeal barrier (BLMB) were chosen throughout the cortical meninges.

Table 1
Overview of immunohistochemical analysis. Analyses of BBB and BLMB was based on paraffin-embedded tissue. BCSFB analyses was performed on cryosections of the choroid plexus.

Marker	Brain barrier	Characterization/ Rationale	Reference
ANXA1	BBB	1. Expression in the endothelial cells – BBB integrity 2. Enumerating circulating leukocytes	(Cristante et al., 2013; McArthur et al., 2016; Gussenhoven et al., 2019) Perretti and D'Acquisto (2009)
	BLMB	Enumerating circulating leukocytes	Perretti and D'Acquisto (2009)
	BCSFB	Enumerating circulating leukocytes (CD45 co-stain) and determining expression level in leukocytes	Perretti and D'Acquisto (2009)
CD45	BBB, BLMB & BCSFB	Enumerating circulating leukocytes and leukocytes present within the brain parenchyma, co-staining with ANXA1 in BCSFB	Jeong et al. (2013)
	BCSFB	Enumerating circulating leukocytes, co-staining with ANXA1	Jeong et al. (2013)
Myeloperoxidase (MPO)	BBB, BLMB & BCSFB	Enumerating circulating neutrophils	Jeong et al. (2013)
IBA-1	BBB & BLMB	Enumerating circulating monocytes	Jeong et al. (2013)
CD206	BCSFB	Enumerating barrier associated macrophage marker, (ANXA1 co-stain), anti-inflammatory macrophage marker	Jurga et al. (2020)

2.6.2. *Immunohistochemistry of paraffin-embedded sections*

The brain was halved along the midline and each hemisphere was further dissected coronally into 5 mm-thick blocks. Blocks from the left cerebral hemisphere were snap-frozen in liquid nitrogen individually, while those from the right cerebral hemisphere were immersion-fixed in 4% paraformaldehyde in 0.1 M phosphate buffer (pH 7.4), processed through alcohol and xylene washes and embedded in paraffin wax. 4 μm sections from each brain region (Fig. 2) were cut with a microtome (Leica RM2235, Leica Microsystems, Wetzlar, Germany). Immunohistological staining was performed on mainly adjacent slides within the regions of interest (Fig. 2) of each fetal brain. Circulating immune cells and immune cells within the brain parenchyma were assessed by staining for leukocyte common antigen (CD45) (1:1000, monoclonal mouse IgG1 anti-sheep CD45, MCA2220GA, Bio-Rad) and ANXA1 (1:300, polyclonal rabbit anti-ANXA1, ab137745, Abcam). Ionized calcium-binding adaptor protein (IBA-1) (1:1000, polyclonal rabbit anti-IBA-1, 019–19741, Wako Pure Chemical Industries, Osaka, Japan) expressed in round cells within the circulation was used as a marker for monocytes (Jeong et al., 2013). The quantity of circulating neutrophils was assessed by the immunohistochemical marker myeloperoxidase (MPO) (1:200, polyclonal rabbit anti-human MPO, A0398, DAKO Agilent Technologies, Santa Clara, CA) (Jeong et al., 2013). Deparaffinization and rehydration was performed by incubation in xylol and decreasing alcohol concentrations. Endogenous peroxidase activity was blocked by incubation in 0.3% H_2O_2 diluted in phosphate buffered saline (pH 7.4) (CD45, IBA-1, MPO) or 0.3% H_2O_2 diluted in TBS (pH 7.4) (ANXA1) for 20 min. Antigen retrieval for CD45, IBA-1 and ANXA1 involved boiling tissues in 10 mM citrate buffer (pH 6.0) for a total of 10 min. Non-specific binding was prevented by incubation with 4% normal goat serum for 1 h. Tissues were incubated with the primary antibody in a humidified box at 4 °C overnight. MPO was incubated with PBS supplemented with 0.1% Triton X-100. Overnight incubation was followed with the secondary antibody at 1:200 (polyclonal goat anti-mouse biotin, E0433, DAKO (CD45), polyclonal swine anti-rabbit biotin, E0353, DAKO (IBA-1, ANXA1) or 1:50 (polyclonal goat anti-rabbit HRP, 111-035-045, Jackson ImmunoResearch, West Grove, PA (MPO)) for 1 h at room temperature. For CD45, IBA-1 and ANXA1 the antigen-specific signal was enhanced with a Vectastain ABC peroxidase Elite kit (Vector Laboratories Inc., Burlingame, CA) for 1 h and 3,3′-diaminobenzide (DAB) for 1–4 min. Tissues were incubated with Mayer's haematoxylin followed by dehydration increasing alcohol concentrations and xylol.

2.7. *Qualitative and semi-quantitative analyses*

The researchers performing the analyses were blinded for the experimental conditions. Paraffin-embedded slides were scanned using a light microscope at 200x or 400x magnification (Ventana iScan, Ventana Medical System, Inc., Tucson, AZ). Analyses were performed using QuPath v0.2.0-m8 (Prame Kumar et al., 2018). For integrated density measurements of ANXA1 in endothelium, ten blood vessels of the same size located within the white matter tracts per brain section of interest were annotated and analyzed. An estimated stain vector was

created, to set the detection limit. A pixel classifier was set based on representative DAB positive, DAB negative cells and background to determine the DAB-mean value and DAB stained area (area fraction). The DAB-mean value (0.0–1.0) was corrected by multiplying with 255 and subtraction from 255 to create a positive correlation between a high DAB intensity resulting in a corrected mean grey value. Integrated density was calculated by multiplying the area fraction by the corrected mean grey value. Consequently, a higher mean integrated density indicates a higher expression of ANXA1 within the endothelium. For quantification of circulatory cells ($CD45^+$, $ANXA1^+$, MPO^+ or $IBA\text{-}1^+$), 10 vessels at magnification of 200x of both the parenchyma and meninges were analysed in adjacent sections. Positive cells were counted and expressed as total cell count per square millimetre (cells/mm^2). Additionally, $CD45^+$ and $ANXA1^+$ cells, having a round morphology and lacking processes (see Fig. 4B, D), in the brain parenchyma within close proximity to a blood vessel were analysed. Per animal, ten squares of 0.77 mm^2 excluding the area of the blood vessel were quantified per brain region. The data (for circulatory immune cells at the BBB and BLMB, cerebrovascular ANXA1 expression and $CD45^+$ or $ANXA1^+$ cells within the brain parenchyma) of all three brain regions (frontal, striatal and hippocampal region) were averaged as no region differences were observed. For the fluorescent (co-) staining (CD45/ANXA1, CD206/ANXA1, MPO) of the frozen sections, ten images of the choroid plexus per animal were taken by a confocal microscope (Leica DMI 4000, Leica Microsystems) at 400x magnification. (Co-)stained cells were counted manually and expressed per tissue area (mm^2) measured by QuPath v0.2.0-m8 (Bankhead et al., 2017). $CD45^+$ cells were labelled as monocyte or neutrophil based on morphology (see Figs. S2 and S4). Quantity of monocyte and neutrophil populations per image were as well subjectively ranked on a 0–3 score with a higher score indicating more cells per image (see Fig. S3 A, B). For subjective scoring of level of ANXA1 expression in $CD45^+$ cells an intensity score from 0 to 3 was used (see Fig. S4). To quantify ANXA1 expression in $CD45^+$ and $CD206^+$ cells, double positive cells were further analysed by measuring the integrated density (IntDen) (mean grey value * area) of $ANXA1^+$ using ImageJ (National Institutes of Health, Bethesda, MD) including a threshold of 25 mean grey scale value for CD206, CD45 and ANXA1.

2.8. Statistical analysis

All statistical analyses were performed in GraphPad Prism (version 6.01; GraphPad; San Diego, CA). All values were computed per animal as mean and standard deviation. For the IL-6 data two-way repeated measures ANOVA was performed with a Turkey's multiple comparisons test at different time points (Fig. 3) and between treatment groups was performed (p values reported within text). For timely follow-up of IL-6 levels, two separate tests were performed including 125–127 day of gestation for LPS effect and 127–132 days of gestation for the MAPC effect. Statistical differences for immunohistochemical stainings were confirmed by performing a two-way ANOVA with a Turkey's multiple comparisons test. Statistical significance was set at alpha = 0.05. Results of the overall two-way ANOVA are reported with \$ $p < 0.05$, \$\$ $p < 0.01$, \$\$\$ $p < 0.001$, \$\$\$\$ $p < 0.0001$ for an interaction effect of LPS and MAPC, § $p < 0.05$, §§ $p < 0.01$, §§§ $p < 0.001$, §§§§ $p < 0.0001$ for a LPS effect (row factor), and £ $p < 0.05$, ££ $p < 0.01$, £££ $p < 0.001$, ££££ $p < 0.0001$ indicates a MAPC effect (column factor). Significant differences of the Turkey's multiple comparison test are illustrated by *$p < 0.05$, **$p < 0.01$, ***$p < 0.001$, ****$p < 0.0001$, and #$p < 0.1$ is considered an effect with possible biological relevance.

3. Results

3.1. I.a. LPS induces an acute increase of systemic IL-6 and i.v. MAPCs increases cerebrovascular ANXA1 in LPS-exposed animals

At 126 days of gestation, LPS induced a significant increase in plasma IL-6 levels 24 h after administration, prior to MAPC or SAL treatment (at 24 h: SAL-SAL vs LPS-SAL p = 0.04, SAL-SAL vs LPS-MAPC p = 0.004, SAL-MAPC vs LPS-SAL p = 0.03; SAL-MAPC vs LPS-MAPC p = 0.003, Fig. 3). Systemic IL-6 levels normalized from 48 h after i.a. LPS exposure onwards (Fig. 3). 24 and 48 h after MAPC administration did not induce an increase in plasma IL-6 levels (Fig. 3). In addition, we evaluated whether LPS exposure and MAPC treatment led to changes within the cerebrovasculature in terms of endogenous endothelial ANXA1 expression as a BBB integrity marker (Cristante et al., 2013; McArthur et al., 2016; Gussenhoven et al., 2019). ANXA1 expression was upregulated in endothelial cells of the BBB in LPS-MAPC animals compared to SAL-SAL, LPS-SAL and SAL-MAPC animals (Fig. 3, \$: F = 8.16, p = 0.009; §: F = 3.19, p = 0.089; £: F = 3.88, p = 0.062).

3.2. $CD45^+$ and ANXA1+ cells extravasate in the brain parenchyma in LPS-MAPC exposed animals

Previously, macrophage-like cells around cerebral blood vessels were observed after systemic inflammation in fetal sheep, suggesting that peripheral immune cells extravasated into the neonatal brain parenchyma (Yan et al., 2004). Thus, we enumerated $CD45^+$ and $ANXA1^+$ cells in the brain parenchyma and found significant higher amounts of CD45 (Fig. 4A, \$: F = 10.27, p = 0.004; §: F = 7.63, p = 0.012; £: F = 13.15, p = 0.002) and ANXA1 (Fig. 4C, \$: F = 20.67, p = 0.0002; §: F =

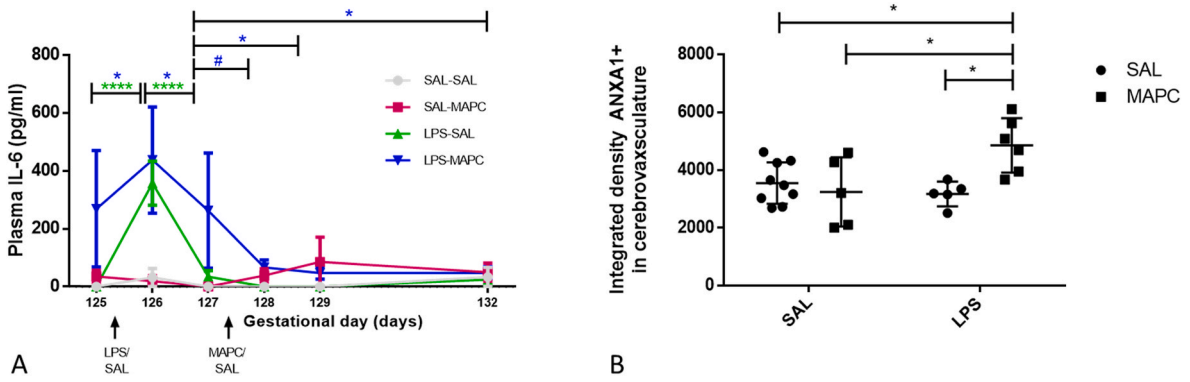

Fig. 3. Systemic IL-6 levels and cerebrovascular ANXA1 expression after i.a. LPS and stem cell treatment. A) Time course of fetal blood plasma IL-6 levels (pg/mL) after i.a. LPS exposure and MAPC treatment. Fetal blood plasma on day 125 and 127 were taken before i.a. LPS/SAL and MAPC/SAL administration, respectively. Results of the two-way repeated measures ANOVA and post-test are indicated with: *p < 0.05, **p < 0.01, ***p < 0.001, ****p < 0.0001, #<0.1. B) Average of integrated density (mean grey value of stained area*percentage of stained area) of endogenous ANXA1 expression in cerebrovasculature in coronal brain sections 1, 2 and 3. Summary of the ANOVA results are presented on each panel (effects of interaction between LPS and MAPCs [INTx, \$], effects of LPS [LPS, §] and effects of MAPCs [MAPCs, £]). Results of the post-test are indicated with: *p < 0.05, **p < 0.01, ***p < 0.001, ****p < 0.0001.

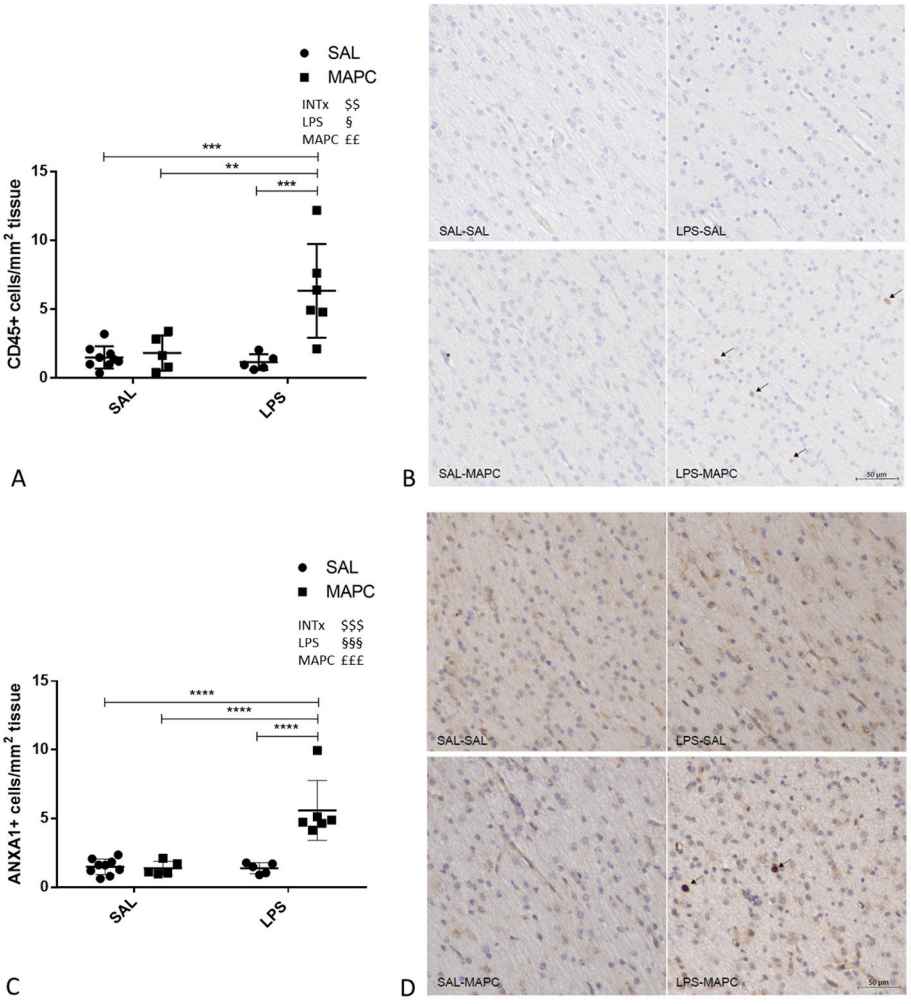

Fig. 4. CD45$^+$ and ANXA1$^+$ cells per mm^2 brain parenchyma. A) Quantification of CD45$^+$ cells per mm^2 brain parenchyma throughout the cerebrum; B) Representative pictures of CD45 expressing round cells within the brain parenchyma, arrows indicate cells within the tissue. C) Quantification of ANXA1$^+$ cells per mm^2 brain parenchyma throughout the cerebrum; D) Representative pictures of ANXA1$^+$ expressing round cells within the brain parenchyma, arrows indicate cells within the tissue. Summary of the ANOVA results are presented on each panel (effects of interaction between LPS and MAPCs [INTx, $], effects of LPS [LPS, §] and effects of MAPCs [MAPCs, £]). Results of the post-test are indicated with: *p < 0.05, **p < 0.01, ***p < 0.001, ****p < 0.0001. Scale bar 50 μm, magnification 400x.

18.69, p = 0.0003; £: F = 18.66, p = 0.0003) expressing round cells in the brain parenchyma of animals that received i.a. LPS and i.v. MAPC treatment. Fig. 4B and D shows typical morphology of round CD45$^+$ and ANXA1$^+$ cells.

3.3. Antenatal inflammation and i.v. MAPC treatment increase BBB-associated ANXA1 expressing cells and immune cells, particularly monocytes and neutrophils at the BBB and BLMB

ANXA1 does not only play a role in BBB integrity regulation (Fig. 3B), it is also highly expressed in monocytes and neutrophils (Perretti and D'Acquisto, 2009). We found higher numbers of round leukocyte-like ANXA1 expressing cells accumulating at the BBB throughout the cerebrum (frontal, striatal, hippocampal region) in animals exposed to i.a. LPS and MAPC treatment compared to all other groups (Fig. 5, $: F = 8.45, p = 0.008; §: F = 11.25, p = 0.003; £: F = 17.60, p = 0.0004, Fig. S1). Similarly, ANXA1 expressing cells accumulated at the BLMB in animals exposed to i.a. LPS and MAPC treatment compared to all other groups (Fig. 6, $: F = 3.01, p = 0.093; §: F = 2.21, p = 0.152; £: F = 11.42, p = 0.003). The BBB and BLMB represent potential entry and communication portals of peripheral immune cells to the CNS even though the endothelial cells are closely connected through tight junctions (Shechter et al., 2013a). To investigate whether ANXA1$^+$ cells could be leukocytes, we enumerated CD45$^+$ expressing cells at the BBB (Fig. 5, $: F = 20.20, p = 0.0002; §: F = 24.60, p < 0.0001; £: F = 35.35, p < 0.0001; Fig. S1) and BLMB (Fig. 6, $: F = 2.49, p = 0.129; §: F = 8.68, p = 0.008; £: F = 14.36, p = 0.001), mirroring the results of ANXA1$^+$ cells. Further characterizing immune cells showed that leukocyte-like cells mainly consisted out of monocytes (IBA-1$^+$) and neutrophils (MPO$^+$) accumulating at the BBB (Fig. 5, IBA-1: $: F = 0.87, p = 0.361; §: F = 0.95, p = 0.341; £: F = 11.40 p = 0.003; MPO: $: F = 15.70, p = 0.0007; §: F = 15.36, p = 0.0008; £: F = 25.86, p < 0.0001, Fig. S1) and the BLMB (Fig. 6, IBA-1: $: F = 1.98, p = 0.174; §: F = 1.73, p = 0.203; £: F = 12.63, p = 0.002; MPO: $: F = 6.62, p = 0.018; §: F = 5.89, p = 0.024; £: F = 10.16, p = 0.004) throughout the cerebrum in the LPS-MAPC experimental group.

3.4. I.a. LPS and i.v. MAPC treatment causes accumulation of CD45$^+$ immune cells consisting of neutrophils and choroid plexus macrophages/monocytes at the BCSFB

As the choroidal BCSFB is a predominant site of leukocyte crossing in neuroinflammation and has previously been shown to act as actively recruiting and educative gate in adult and neonatal inflammatory diseases (Schwartz and Baruch, 2014; Mottahedin et al., 2019; Szmydynger-Chodobska et al., 2009, 2012; Rayasam et al., 2020), we enumerated CD45$^+$ immune cells at the choroid plexus.

Seven days after fetuses were exposed to i.a. LPS and 5 days after i.v. MAPC treatment we found a some 2-fold increase of CD45$^+$ immune cells at the choroid plexus compared to control groups (SAL-SAL, SAL-MAPC) and non-treated LPS exposed fetuses (LPS-SAL) (Fig. 7A and B, $: F = 4.81, p = 0.040; §: F = 8.52, p = 0.009; £: F = 7.73, p = 0.012). CD45$^+$ immune cells exhibited a monocyte/macrophage-like morphology or neutrophil-like morphology (Figs. S2A and B). To

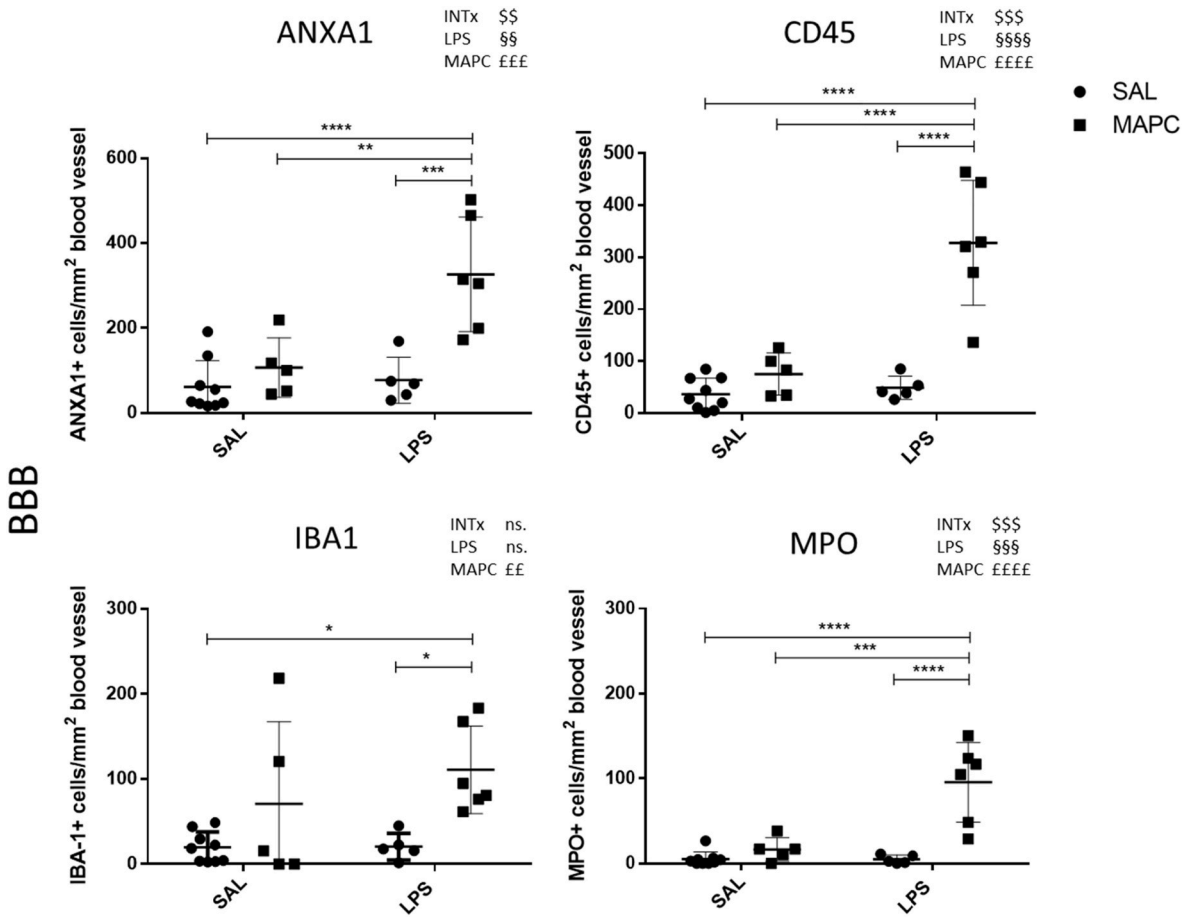

Fig. 5. Quantification of ANXA1$^+$, CD45$^+$, IBA-1$^+$ and MPO$^+$ per mm^2 blood vessel of the BBB throughout the cerebrum after i.a. LPS and i.v. MAPC treatment. Summary of the ANOVA results are presented on each panel (effects of interaction between LPS and MAPCs [INTx, $], effects of LPS [LPS, §] and effects of MAPCs [MAPCs, £]). Results of the post-test are indicated with: *p < 0.05, **p < 0.01, ***p < 0.001, ****p < 0.0001.

further characterize CD45$^+$ cells at the BCSFB we counted CD206$^+$ cells, previously described as (BCSFB, meningeal barrier, perivascular macrophages) at the choroid plexus (Goldmann et al., 2016), and MPO$^+$ cells. In line, with the amount of CD45$^+$ immune cells, CD206$^+$ immune cells in the LPS-MAPC group increased compared to control groups (SAL-SAL, SAL-MAPC) and non-treated LPS exposed (LPS-SAL) animals (Fig. 7C and D, $: F = 5.481, p = 0.030; §: F = 10.97, p = 0.004; £: F = 7.83, p = 0.011). Similar, patterns were detected for MPO$^+$ cells which increased some 6-fold in the LPS-MAPC animals compared to the non-treated LPS exposed fetuses (LPS-SAL) or controls (SAL-SAL, SAL-MAPC) (Fig. 7E and F, $: F = 26.57, p < 0.0001; §: F = 32.95, p < 0.0001; £: F = 36.76, p < 0.0001). Similar, trends were obtained with subjective scoring for monocyte/macrophage-like cells (Fig. S3A, $: F = 10.24, p = 0.005; §: F = 3.52, p = 0.075; £: F = 8.76, p = 0.008) and neutrophil-like cells (Fig. S3B, $: F = 13.42, p = 0.002; §: F = 14.32, p = 0.001; £: F = 16.46, p = 0.0006). These findings suggest that the main contributors to the increase in CD45$^+$ immune cells 7 days after antenatal inflammation and 5 days after stem cell treatment at the BCSFB are neutrophils and monocytes/barrier-associated macrophages.

3.5. Immune cells at the BCSFB exhibit decreased ANXA1 expression after antenatal inflammation which is restored and enhanced upon MAPC treatment

As neutrophils and monocytes/macrophages act as partners in crime in resolution of inflammation through the action of ANXA1 (Prame Kumar et al., 2018; Sugimoto et al., 2016), we quantified expression of ANXA1 in CD45$^+$ cells.

ANXA1 and CD45 co-localized at the choroid plexus in cells exhibiting the morphology of resident choroid plexus macrophages (CD206) and peripheral immune cells such as neutrophils and monocytes (Fig. 8B, Figs. S4 and S5B). In line with previous results, we found in LPS-MAPC treated animals some 2-fold increase of CD45$^+$ANXA1$^+$ cells in choroid plexus compared to LPS untreated fetuses and control groups (SAL-SAL, SAL-MAPC) (Fig. 8A and B, $: F = 10.35, p = 0.004; §: F = 4.74, p = 0.042; £: F = 9.07, p = 0.007). Of note, a similar some 2-fold increase of ANXA1 expressing choroid plexus macrophages in the LPS-MAPC group compared to LPS-SAL group and controls (SAL-SAL, SAL-MAPC) was evident (Figs. S5A and B, $: F = 6.32, p = 0.021; §: F = 7.76, p = 0.011; £: F = 4.20, p = 0.054). Interestingly, while the percentage of ANXA1 expressing CD45$^+$ cells did not significantly change between control groups (SAL-SAL, SAL-MAPC) and LPS-MAPC treated animals (71–83%), the percentage of ANXA1 expressing CD45$^+$ cells in non-treated controls decreased compared to non-treated fetuses exposed to antenatal inflammation (SAL-SAL vs LPS-SAL, 83% vs 60%), a phenomenon partially reversed by MAPC treatment (LPS-MAPC: 81%; Fig. 8C, $: F = 6.91, p = 0.016; §: F = 1.10, p = 0.308; £: F = 0.413, p = 0.528). This finding was accompanied by decreased expression levels of ANXA1 per CD45$^+$ cell in the LPS-SAL group which was restored and even enhanced in LPS-MAPC treated fetuses (Fig. 8D, $: F = 22.41, p = 0.0001; §: F = 0.79, p = 0.385; £: F = 5.62, p = 0.028). These data are in line with subjective scoring of ANXA1 expression in CD45$^+$ immune cells (Fig. S4, $: F = 9.20, p = 0.007; §: F = 0.35, p = 0.559; £: F = 4.92, p = 0.038) and ANXA1 in choroid plexus macrophages (CD206) exhibiting higher intensity scoring of ANXA1 quantification in the LPS-MAPC animals and a lowest ANXA1 expression in the animals exposed to

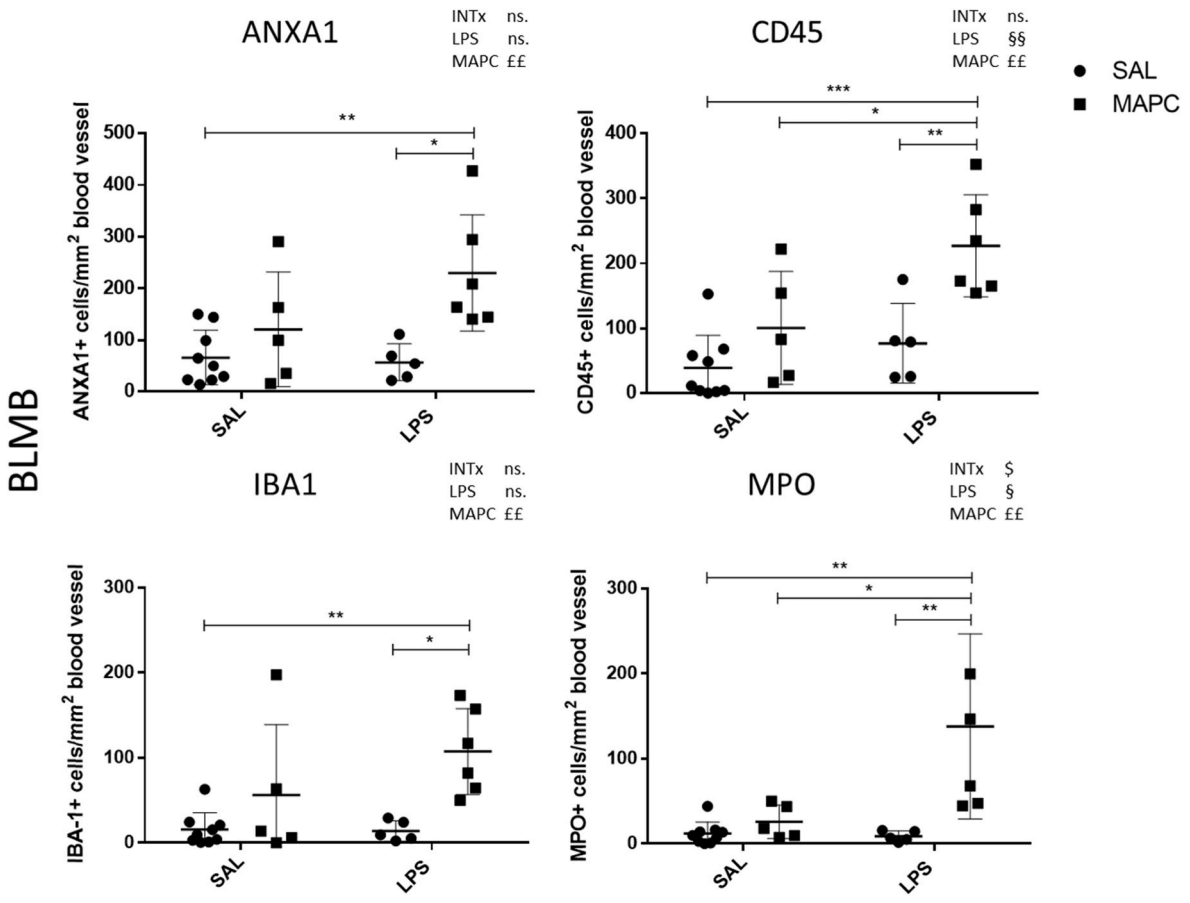

Fig. 6. Quantification of ANXA1$^+$, CD45$^+$, IBA-1$^+$ and MPO$^+$ per mm^2 blood vessel of the BLMB throughout the cerebrum after i.a. LPS and i.v. MAPC treatment. Summary of the ANOVA results are presented on each panel (effects of interaction between LPS and MAPCs [INTx, $], effects of LPS [LPS, §] and effects of MAPCs [MAPCs, £]). Results of the post-test are indicated with: *p < 0.05, **p < 0.01, ***p < 0.001, ****p < 0.0001.

antenatal inflammation without treatment (Fig. S5D, $: F = 4.08, p = 0.050; §: F = 0.81, p = 0.379; £: F = 2.024, p = 0.170).

4. Discussion

In this study we show that i.a. LPS induced an acute systemic inflammatory response indicated by significantly elevated plasma IL-6 levels. Seven days after i.a. LPS exposure ANXA1 levels in the endothelium of cerebrovasculature, as readout for BBB integrity (Cristante et al., 2013; McArthur et al., 2016; Gussenhoven et al., 2019), remained stable and presence of barrier associated immune cells was comparable to control groups (SAL-SAL, SAL-MAPC). Despite only few indications of an LPS effect on neuroinflammation at the studied timepoint, the combination of antenatal inflammation and prenatal *in utero* MAPC treatment upregulated endogenous ANXA1 in cerebrovasculature and prevented LPS-induced loss of the anti-inflammatory phenotype of the peripheral immune cells towards the brain in an ovine chorioamnionitis model.

In terms of the temporal course of cerebrovascular ANXA1 expression and systemic inflammation (i.e. circulating IL-6 levels), our study confirms previous findings in a fetal ovine chorioamninoitis model (Gussenhoven et al., 2017, 2018; Ophelders et al., 2020). In this LPS kinetics study, we detected an acute decrease of ANXA1 expression at two to four days after i.a. LPS exposure, which was restored to baseline levels eight days after the infectious trigger (Ophelders et al., 2020). Stem cells or stem cell-based therapies have been previously shown to preserve BBB integrity after an injurious hit (Yawno et al., 2013; Walker et al., 2010; Gussenhoven et al., 2019). Enhanced cerebrovascular ANXA1 expression in LPS exposed and MAPC treated animals could therefore indicate a compensatory effect induced by MAPCs in the inflammatory milieu to strengthen BBB integrity (Cristante et al., 2013) or to limit leukocyte trafficking (Maggioli et al., 2016). In terms of systemic inflammation, we recently reported an acute systemic IL-6 response (12h–24h) after i.a. LPS exposure in an ovine model for chorioamnionitis (Gussenhoven et al., 2017, 2018). In these studies, the systemic response was paralleled by immediate microgliosis 12 h up to four days after exposure to i.a. LPS that normalized to control seven days or eight days after LPS exposure (Gussenhoven et al., 2017, 2018). MPO$^+$ cells were unchanged at the BCSFB or within the brain parenchyma 5 h up to eight days after LPS exposure. However, 15 days after LPS exposure, MPO$^+$ cells were to a greater extend evident in the white matter, accompanied by increased apoptosis and oligodendrocyte loss (Gussenhoven et al., 2018). Taken together, previous studies strongly suggest that i.a. LPS administration induces systemic inflammation leading to neuroinflammation and subsequent brain injury. Thus, administration of MAPCs occurred during a phase of extenuating systemic inflammation and abundant neuroinflammation.

In previous studies, human amnion epithelial cells were neuroprotective in an ovine model for chorioamnionitis, by decreasing microgliosis and improvement of the BBB integrity (Yawno et al., 2013). Other studies validated the neuroprotective, anti-inflammatory and BBB protective effects of stem cells after neonatal inflammation by attenuation of apoptosis, neuroinflammation and loss of oligodendrocyte lineage cells (Yawno et al., 2017; Paton et al., 2018, 2019). Collectively, this suggest that stem cell treatment improves brain outcome by modulation of neuroinflammation. As neuroinflammation in FIRS is perpetuated by systemic inflammation, we focussed on the periphery to brain directed immune response which is a missing link in the mechanisms of adult

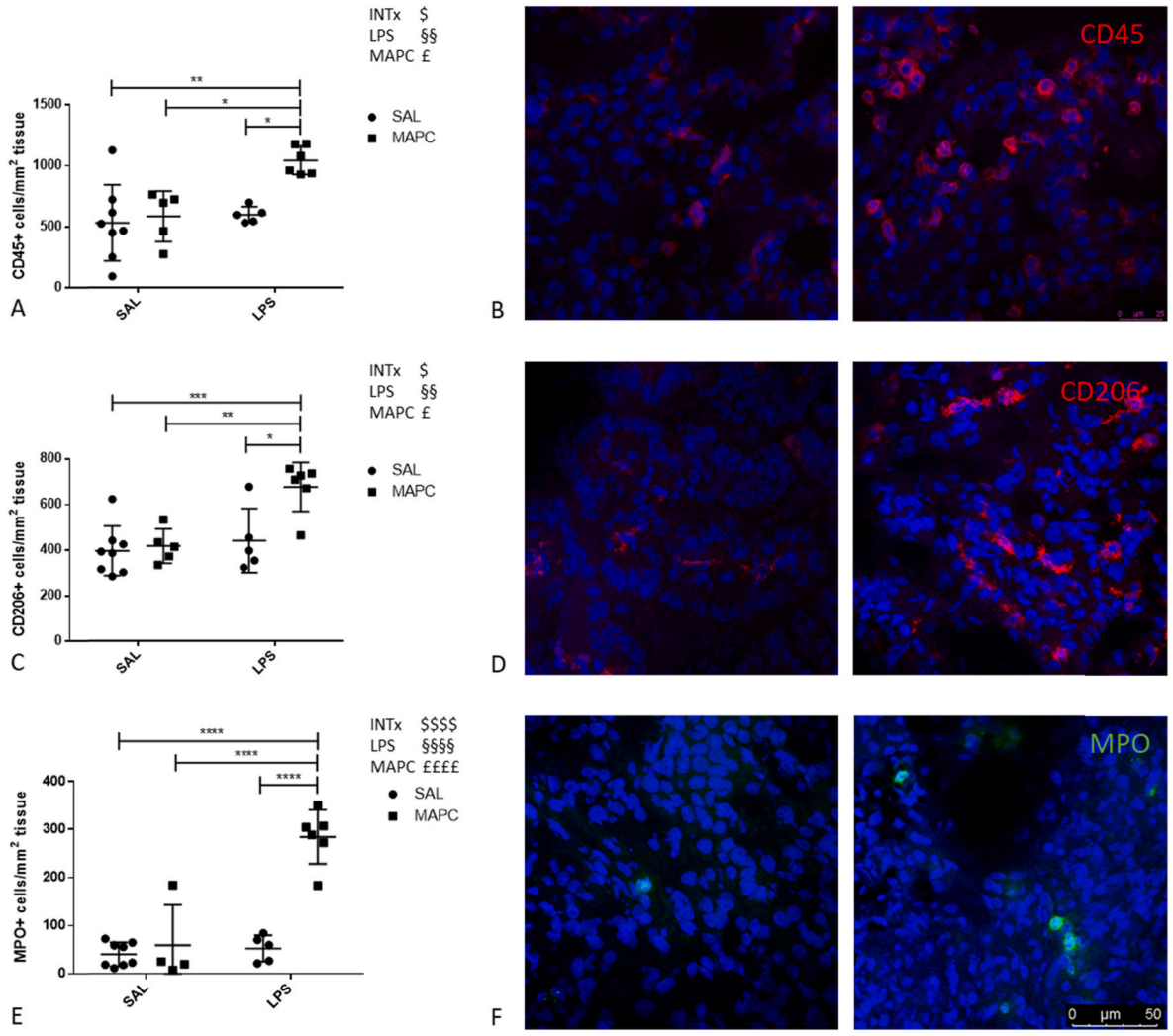

Fig. 7. Characterization of immune cells at the BCSFB after antenatal inflammation and stem cell treatment. A) Amount of $CD45^+$ cells (immune cells) per mm^2 at the choroidal BCSFB; B) Representative picture of $CD45^+$ staining at the choroid plexus for LPS-SAL (left panel, SAL-SAL and SAL-MAPC were comparable to LPS-SAL) and LPS-MAPC treated animals (right panel), CD45 (red), DAPI (blue); C) Amount of $CD206^+$ cells (barrier associated macrophages) per mm^2 at the choroidal BCSFB; D) Representative picture of $CD206^+$ staining at the choroid plexus for SAL-SAL, SAL-MAPC and LPS-SAL (left panel) and LPS-MAPC treated animals (right panel), CD206 (red), DAPI (blue); E) Amount of MPO^+ cells (neutrophils) per mm^2 at the choroidal BCSFB; F) Representative picture of MPO^+ staining at the choroid plexus for SAL-SAL, SAL-MAPC and LPS-SAL (left panel) and LPS-MAPC treated animals (right panel), MPO (green), DAPI (blue). Summary of the ANOVA results are presented on each panel (effects of interaction between LPS and MAPCs [INTx, $], effects of LPS [LPS, §] and effects of MAPCs [MAPCs, £]). Results of the post-test are indicated with: *$p < 0.05$, **$p < 0.01$, ***$p < 0.001$, ****$p < 0.0001$. Scale bar 50 µm, magnification 400x.

stem cell therapy.

Previous studies in a sepsis model of neonatal rats indicate that stem cells affect the CNS by reducing neuroinflammation via modulation of the systemic immune response, resulting in improved functional brain outcome after an infectious trigger (Sato et al., 2020; Abe et al., 2020). Importantly, the prophylactic intraperitoneal delivered human amniotic fluid stem cells did not migrate towards the brain (Sato et al., 2020), which supports the hypothesis that improved cognitive outcome is linked to immunomodulation of the periphery. In line, *in vivo* models for traumatic brain injury showed that direct contact of MAPCs with the splenocytes is necessary to preserve BBB integrity and induce a neuroprotective microglial phenotype, indicating an important role of MAPCs in influencing neuroimmune crosstalk over brain barriers to protect the brain (Walker et al., 2010, 2012).

Modulation of the neuroimmune axis solely occurred in the animals that received MAPCs in an inflammatory environment (LPS-MAPC) demonstrated by accumulation of barrier-associated macrophages, circulating neutrophils and monocytes at the BCSFB, BBB and BLMB and increased $CD45^+$ and $ANXA1^+$ cells within the cerebral parenchyma, which possibly represent extravasated leukocytes (Jeong et al., 2013; Engelhardt et al., 2017; Prinz and Priller, 2017). The choroid plexus/BCSFB is an active recruitment and entry site of monocytes and neutrophils and may potentiate recruitment of immune cells with an anti-inflammatory phenotype in response to brain injury (Schwartz and Baruch, 2014; Shechter et al., 2013b; Mottahedin et al., 2017, 2019). In line, systemic inflammation induced by LPS in neonatal rodents did not cause significant cell trafficking at the choroid plexus and extravasation of leukocytes into brain parenchyma even though the systemic response was significantly elevated (Mottahedin et al., 2017, 2019). Timing of our end point analysis might be responsible for this finding as discussed before. Though, the increased recruitment of leukocytes to the brain barriers and into the tissue in the LPS-MAPC group underscores the immunomodulatory role of MAPCs in an inflammatory environment. MAPCs respond differently and exert enhanced therapeutic potential when exposed to an inflammatory environment which explains the absence or less pronounced MAPC effects in sham animals (Le Blanc and Mougiakakos, 2012; Le Blanc and Davies, 2015; Li and Hua, 2017; Uccelli et al., 2008; Ravanidis et al., 2017).

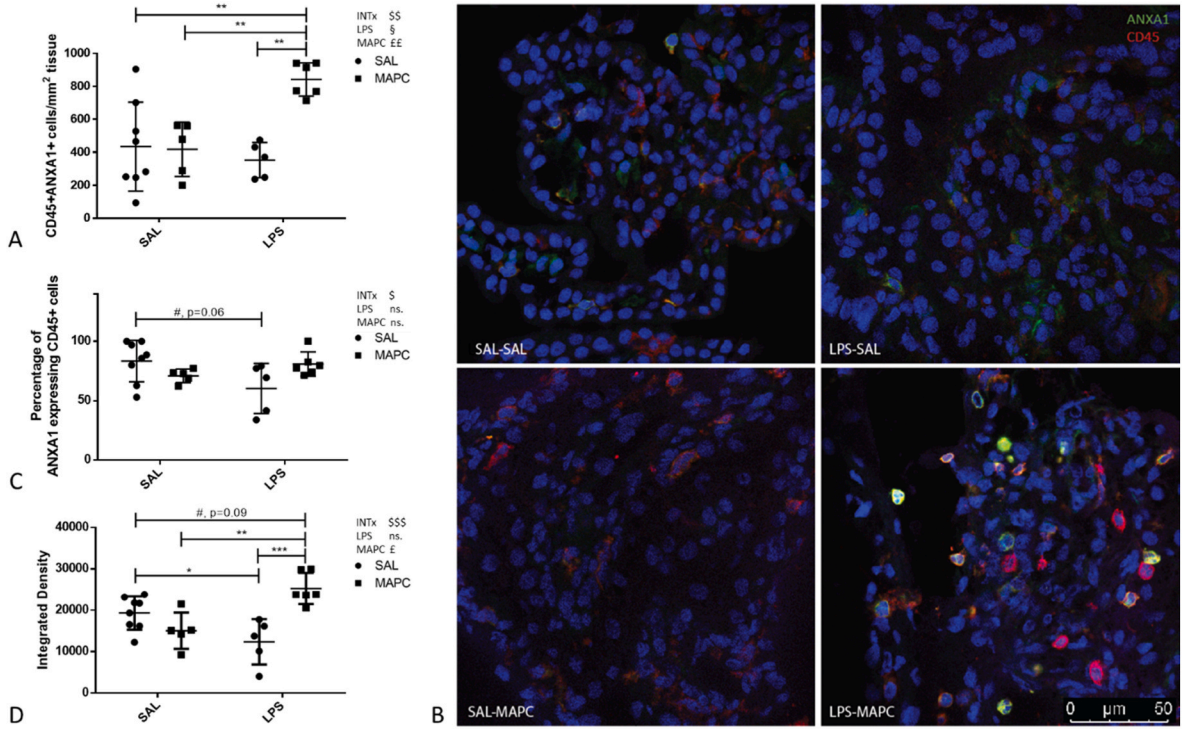

Fig. 8. CD45$^+$ANXA1$^+$ cells at the BCSFB after antenatal inflammation and stem cell treatment. A) Quantification of ANXA1 expressing CD45$^+$ cells per mm^2 tissue area; B) Representative pictures of ANXA1 and CD45 co-staining per treatment group, scale bar 50 µm, 400x magnification, CD45 (red), ANXA1 (green); C) Percentage of ANXA1 expressing CD45$^+$ cells per mm^2 tissue area at the choroid plexus, # indicates a trend (p = 0.06). D) Quantification of ANXA1 expression level in CD45$^+$ cells, # indicates a trend (p = 0.09). Summary of the ANOVA results are presented on each panel (effects of interaction between LPS and MAPCs [INTx, $], effects of LPS [LPS, §] and effects of MAPCs [MAPCs, £]). Results of the post-test are indicated with: *p < 0.05, **p < 0.01, ***p < 0.001, ****p < 0.0001, $p < 0.1$ is considered a trend, which is illustrated by #.

Adult stem cells have been shown in preclinical models to protect from sepsis/infections (Khan and Newsome, 2019). MSCs protect against sepsis by enhancement of the phagocytic activity of neutrophils and macrophages, and release of anti-bactericidal peptides (Khan and Newsome, 2019). In a spinal cord injury model, MAPC treatment was associated with reduced urinary tract infections (Jones et al., 2019). Stem cells can directly influence the innate immune system through secretion of paracrine factors or direct cell-to-cell contact. They can elongate survival of neutrophils, guide neutrophils to the site of injury/infection by IL-6 secretion, decreased spillage of toxic cargo, and direct macrophages into an anti-inflammatory, regenerative phenotype thereby preventing tissue damage/chronic inflammation (Le Blanc and Mougiakakos, 2012; Le Blanc and Davies, 2015; Jiang et al., 2016; Raffaghello et al., 2008). Direct and trans-well cultures of MAPC and macrophages/microglia demonstrated that direct and indirect contact is sufficient enough for immunomodulation of macrophages to dampen their inflammatory response and in turn render the expression profile of MAPCs, indicating a reciprocal communication between innate immune cells and MAPCs (Ravanidis et al., 2017). In a sepsis model, i.v. injected MSCs increased the number of circulating neutrophils while decreasing neutrophils in tissue and circulating monocytes and inducing predominantly pulmonary macrophages with M2 phenotype thereby improving overall survival (N é meth et al., 2009). This suggests the ability of MSCs to modulate circulating and tissue-bound innate immune cells in order to increase the bactericidal potential without induction of organ injury. Balancing the immune response is one therapeutic action of stem cells and mechanisms how it works is still topic of ongoing research (Bennet et al., 2018).

Downstream effectors balancing inflammation after stem cell treatment remain largely unknown; however, a potential candidate is the pro-resolving ANXA1. The small molecule was identified as key player for regenerative effects of stem cell therapy in pancreatic, hepatic and pulmonary pathologies (Zagoura et al., 2019; Rackham et al., 2016; Tovar et al., 2020). Recent reports demonstrated tissue protective and regenerative activity of ANXA1 in brain, heart, liver and skeletal muscle (McArthur et al., 2010, 2020; Ferraro et al., 2019; Locatelli et al., 2014; Ries et al., 2016). The main source of pro-resolving ANXA1 comes from neutrophils that migrate into the inflamed tissue in response to inflammatory signals (Ferraro et al., 2019; McArthur et al., 2020). Here we provide evidence that immune cells, neutrophils and monocytes/barrier associated macrophages, at the choroid plexus express lower levels of ANXA1 seven days after i.a. infection, which is reversed and even enhanced by MAPC treatment. Consistently, the percentage of ANXA1 expressing leukocytes was decreased after i.a. LPS exposure which was reversed by subsequent MAPC treatment. The enhanced immune activation and recruitment of ANXA1 expressing leukocytes to brain barriers and brain could indicate regulation of inflammation which is steered by MAPCs upon *in vivo* licensing by systemic inflammation. This could support timely resolution of inflammation to prevent harmful hyper-inflammation with maintenance of sufficient immunological protection (Schwartz and Baruch, 2014; Bennet et al., 2018).

The neonatal immune response differs from the adult one and is characterized by impaired opsonization and phagocytosis of pathogens, defective synthesis of granulocyte-macrophage stimulating factor, and reduced numbers of macrophages, dendritic cells and neutrophils, which are the first line defenders (Helmo et al., 2018; van Well et al., 2017; Sabic and Koenig, 2020). Chorioamnionitis can induce hypo-responsiveness in monocytes to subsequent infection that causes higher susceptibility for neonatal infections/sepsis later in life (de Jong et al., 2018). Contrarily, chorioamnionitis was associated with an exaggerated immune response when exposed to a secondary inflammatory hit (Sabic and Koenig, 2020; Yellowhair et al., 2019), indicating that *in utero* injury primes the immune system and augments enhanced inflammatory signaling. MAPCs could be beneficial in supporting the

immune system due to their adaptation to the microenvironment to keep the right balance between inflammation and prevention of tissue damage. ANXA1, as a regulator of leukocyte trafficking, could play a crucial role in these processes (Perretti and D'Acquisto, 2009). Whether MAPC treatment thereby renders immune response in later life leading to improved organ outcome remains unclear and needs to be determined in future studies including postnatal hits.

Further future studies are needed to determine the biodistribution to unravel working mechanisms of MAPCs after antenatal inflammation. Similarly, characterization of the peripheral immune response in a longitudinal manner would aid unravel in which direction the immune cells are skewed by antenatal inflammation and MAPC treatment. This could contribute to optimizing therapy for antenatal inflammation by identifying cellular and molecular targets for (adjuvant) therapy e.g. ANXA1 and to define the most optimal treatment window for MAPCs.

5. Conclusion

In conclusion, this study reveals promising insights into possible working mechanisms of i.v. MAPC treatment in regulating neonatal systemic inflammation and modulating brain barriers. We propose that MAPCs in an inflammatory environment modulate the innate immune response and potentially reinforce brain barrier integrity, indicated by enhanced ANXA1 expression. Potentially this could be a MAPC-mediated defence mechanism to induce resolution of inflammation with preserved immunological protection to protect the brain from cumulative inflammatory events in the neonatal period and chronic inflammation (Schwartz and Baruch, 2014; Bennet et al., 2018).

Funding

This work was supported by the Lung Foundation Netherlands (Longfonds, Grant no. 6.1.16.088, TW).

Declaration of competing interest

Multipotent adult progenitor cells were provided by Athersys Inc, Cleveland, Ohio. Athersys Inc. was not involved in the experimental design, (statistical) analysis, data presentation, or decision to publish. CPMR and TGAMW are inventors to a patent application owned by Maastricht University that claims the use of Annexin A1 to treat newborns with hypoxic-ischemic encephalopathy.

Appendix A. Supplementary data

Supplementary data to this article can be found online at https://doi.org/10.1016/j.bbih.2022.100458.

References

Abe, Y., Ochiai, D., Sato, Y., Kanzaki, S., Ikenoue, S., Kasuga, Y., Tanaka, M., 2020. Prophylactic therapy with human amniotic fluid stem cells improves long-term cognitive impairment in rat neonatal sepsis survivors. Int. J. Mol. Sci. 21 https://doi.org/10.3390/ijms21249590.

Börger, V., Bremer, M., Ferrer-Tur, R., Gockeln, L., Stambouli, O., Becic, A., Giebel, B., 2017. Mesenchymal stem/stromal cell-derived extracellular vesicles and their potential as novel immunomodulatory therapeutic agents. Int. J. Mol. Sci. 18 https://doi.org/10.3390/ijms18071450.

Back, S.A., Riddle, A., Dean, J., Hohimer, A.R., 2012. The instrumented fetal sheep as a model of cerebral white matter injury in the premature infant. Neurotherapeutics 9, 359–370. https://doi.org/10.1007/s13311-012-0108-y.

Bankhead, P., Loughrey, M.B., Fernández, J.A., Dombrowski, Y., McArt, D.G., Dunne, P. D., McQuaid, S., Gray, R.T., Murray, L.J., Coleman, H.G., et al., 2017. QuPath: open source software for digital pathology image analysis. Sci. Rep. 7, 16878. https://doi.org/10.1038/s41598-017-17204-5.

Banks, W.A., Gray, A.M., Erickson, M.A., Salameh, T.S., Damodarasamy, M., Sheibani, N., Meabon, J.S., Wing, E.E., Morofuji, Y., Cook, D.G., et al., 2015. Lipopolysaccharide-induced blood-brain barrier disruption: roles of cyclooxygenase, oxidative stress, neuroinflammation, and elements of the neurovascular unit. J. Neuroinflammation 12, 223. https://doi.org/10.1186/s12974-015-0434-1, 223.

Bennet, L., Dhillon, S., Lear, C.A., van den Heuij, L., King, V., Dean, J.M., Wassink, G., Davidson, J.O., Gunn, A.J., 2018. Chronic inflammation and impaired development of the preterm brain. J. Reproduct. Immunol. 125, 45–55. https://doi.org/10.1016/j.jri.2017.11.003.

Blencowe, H., Cousens, S., Oestergaard, M.Z., Chou, D., Moller, A.B., Narwal, R., Adler, A., Vera Garcia, C., Rohde, S., Say, L., et al., 2012. National, regional, and worldwide estimates of preterm birth rates in the year 2010 with time trends since 1990 for selected countries: a systematic analysis and implications. Lancet 379, 2162–2172. https://doi.org/10.1016/S0140-6736(12)60820-4.

Choi, S.-H., Aid, S., Bosetti, F., 2009. The distinct roles of cyclooxygenase-1 and -2 in neuroinflammation: implications for translational research. Trends Pharmacol. Sci. 30, 174–181. https://doi.org/10.1016/j.tips.2009.01.002.

Crabbé, M.A., Gijbels, K., Visser, A., Craeye, D., Walbers, S., Pinxteren, J., Deans, R.J., Annaert, W., Vaes, B.L., 2016. Using miRNA-mRNA interaction analysis to link biologically relevant miRNAs to stem cell identity testing for next-generation culturing development. Stem. Cell. Transl. Med. 5, 709–722. https://doi.org/10.5966/sctm.2015-0154.

Cristante, E., McArthur, S., Mauro, C., Maggioli, E., Romero, I.A., Wylezinska-Arridge, M., Couraud, P.O., Lopez-Tremoleda, J., Christian, H.C., Weksler, B.B., et al., 2013. Identification of an essential endogenous regulator of blood-brain barrier integrity, and its pathological and therapeutic implications. Proc. Natl. Acad. Sci. U S A 110, 832–841. https://doi.org/10.1073/pnas.1209362110.

Cunha, J.P., Leuckx, G., Sterkendries, P., Korf, H., Bomfim-Ferreira, G., Overbergh, L., Vaes, B., Heimberg, H., Gysemans, C., Mathieu, C., 2017. Human multipotent adult progenitor cells enhance islet function and revascularisation when co-transplanted as a composite pellet in a mouse model of diabetes. Diabetologia 60, 134–142. https://doi.org/10.1007/s00125-016-4120-3.

de Jong, E., Hancock, D.G., Wells, C., Richmond, P., Simmer, K., Burgner, D., Strunk, T., Currie, A.J., 2018. Exposure to chorioamnionitis alters the monocyte transcriptional response to the neonatal pathogen Staphylococcus epidermidis. Immunol. Cell Biol. 96, 792–804. https://doi.org/10.1111/imcb.12037.

Doeppner, T.R., Herz, J., Görgens, A., Schlechter, J., Ludwig, A.K., Radtke, S., de Miroschedji, K., Horn, P.A., Giebel, B., Hermann, D.M., 2015. Extracellular vesicles improve post-stroke neuroregeneration and prevent postischemic immunosuppression. Stem cell. Translat.Med. 4, 1131–1143. https://doi.org/10.5966/sctm.2015-0078.

Drommelschmidt, K., Serdar, M., Bendix, I., Herz, J., Bertling, F., Prager, S., Keller, M., Ludwig, A.-K., Duhan, V., Radtke, S., 2017. Mesenchymal stem cell-derived extracellular vesicles ameliorate inflammation-induced preterm brain injury. Brain Behav. Immun. 60, 220–232.

Engelhardt, B., Vajkoczy, P., Weller, R.O., 2017. The movers and shapers in immune privilege of the CNS. Nat Immunol 18, 123–131. https://doi.org/10.1038/ni.3666.

Ferraro, B., Leoni, G., Hinkel, R., Ormanns, S., Paulin, N., Ortega-Gomez, A., Viola, J.R., Jong, R.d., Bongiovanni, D., Bozoglu, T., et al., 2019. Pro-angiogenic macrophage phenotype to promote myocardial repair. J. Am. Coll. Cardiol. 73, 2990–3002. https://doi.org/10.1016/j.jacc.2019.03.503.

Goldmann, T., Wieghofer, P., Jordão, M.J.C., Prutek, F., Hagemeyer, N., Frenzel, K., Amann, L., Staszewski, O., Kierdorf, K., Krueger, M., et al., 2016. Origin, fate and dynamics of macrophages at central nervous system interfaces. Nat. Immunol. 17, 797–805. https://doi.org/10.1038/ni.3423.

Gussenhoven, R., Ophelders, D.R.M.G., Kemp, M.W., Payne, M.S., Spiller, O.B., Beeton, M.L., Stock, S.J., Cillero-Pastor, B., Barré, F.P.Y., Heeren, R.M.A., et al., 2017. The paradoxical effects of chronic intra-amniotic ureaplasma parvum exposure on ovine fetal brain development. Dev. Neurosci. 39, 472–486. https://doi.org/10.1159/000479021.

Gussenhoven, R., Westerlaken, R.J.J., Ophelders, D., Jobe, A.H., Kemp, M.W., Kallapur, S.G., Zimmermann, L.J., Sangild, P.T., Pankratova, S., Gressens, P., et al., 2018. Chorioamnionitis, neuroinflammation, and injury: timing is key in the preterm ovine fetus. J. Neuroinflammation 15, 113. https://doi.org/10.1186/s12974-018-1149-x.

Gussenhoven, R., Klein, L., Ophelders, D., Habets, D.H.J., Giebel, B., Kramer, B.W., Schurgers, L.J., Reutelingsperger, C.P.M., Wolfs, T., 2019. Annexin A1 as neuroprotective determinant for blood-brain barrier integrity in neonatal hypoxic-ischemic encephalopathy. J. Clin. Med. 8 https://doi.org/10.3390/jcm8020137.

Hagberg, H., Mallard, C., Ferriero, D.M., Vannucci, S.J., Levison, S.W., Vexler, Z.S., Gressens, P., 2015. The role of inflammation in perinatal brain injury. Nat. Rev. Neurol. 11, 192–208. https://doi.org/10.1038/nrneurol.2015.13.

Helmo, F.R., Alves, E.A.R., Moreira, R.A.A., Severino, V.O., Rocha, L.P., Monteiro, M., Reis, M.A.D., Etchebehere, R.M., Machado, J.R., Corrêa, R.R.M., 2018. Intrauterine infection, immune system and premature birth. J. Mater. Fetal Neonatal Med: Off. J. Eur. Assoc. Perinatal Med. 31, 1227–1233. https://doi.org/10.1080/14767058.2017.1311318 the Federation of Asia and Oceania Perinatal Societies, the International Society of Perinatal Obstet.

Hu, N., Wang, C., Zheng, Y., Ao, J., Zhang, C., Xie, K., Li, Y., Wang, H., Yu, Y., Wang, G., 2016. The role of the Wnt/β-catenin-Annexin A1 pathway in the process of sevoflurane-induced cognitive dysfunction. J. Neurochem. 137, 240–252. https://doi.org/10.1111/jnc.13569.

Jellema, R.K., Wolfs, T.G., Lima Passos, V., Zwanenburg, A., Ophelders, D.R., Kuypers, E., Hopman, A.H., Dudink, J., Steinbusch, H.W., Andriessen, P., et al., 2013. Mesenchymal stem cells induce T-cell tolerance and protect the preterm brain after global hypoxia-ischemia. PLoS One 8, e73031. https://doi.org/10.1371/journal.pone.0073031.

Jeong, H.-K., Ji, K., Min, K., Joe, E.-H., 2013. Brain inflammation and microglia: facts and misconceptions. Exp Neurobiol 22, 59–67. https://doi.org/10.5607/en.2013.22.2.59.

Jiang, D., Muschhammer, J., Qi, Y., Kügler, A., de Vries, J.C., Saffarzadeh, M., Sindrilaru, A., Beken, S.V., Wlaschek, M., Kluth, M.A., et al., 2016. Suppression of neutrophil-mediated tissue damage-A novel skill of mesenchymal stem cells. Stem cells (Dayton, Ohio) 34, 2393–2406. https://doi.org/10.1002/stem.2417.

Jones, J.M., DePaul, M.A., Gregory, C.R., Lang, B.T., Xie, H., Zhu, M., Rutten, M.J., Mays, R.W., Busch, S.A., Pati, S., 2019. Multipotent adult progenitor cells, but not tissue inhibitor of matrix metalloproteinase-3, increase tissue sparing and reduce urological complications following spinal cord injury. J. Neurotrauma 36, 1416–1427.

Jurga, A.M., Paleczna, M., Kuter, K.Z., 2020. Overview of general and discriminating markers of differential microglia phenotypes. Front. Cell. Neurosci. 14 https://doi.org/10.3389/fncel.2020.00198.

Khan, R.S., Newsome, P.N., 2019. A comparison of phenotypic and functional properties of mesenchymal stromal cells and multipotent adult progenitor cells. Front. Immunol. 10, 1952. https://doi.org/10.3389/fimmu.2019.01952, 1952.

Le Blanc, K., Davies, L.C., 2015. Mesenchymal stromal cells and the innate immune response. Immunology Letters 168, 140–146. https://doi.org/10.1016/j.imlet.2015.05.004.

Le Blanc, K., Mougiakakos, D., 2012. Multipotent mesenchymal stromal cells and the innate immune system. Nat. Rev. Immunol. 12, 383–396.

Li, N., Hua, J., 2017. Interactions between mesenchymal stem cells and the immune system. Cell. Mol. Life Sci.: CMLS 74, 2345–2360. https://doi.org/10.1007/s00018-017-2473-5.

Locatelli, I., Sutti, S., Jindal, A., Vacchiano, M., Bozzola, C., Reutelingsperger, C., Kusters, D., Bena, S., Parola, M., Paternostro, C., et al., 2014. Endogenous annexin A1 is a novel protective determinant in nonalcoholic steatohepatitis in mice. Hepatology 60, 531–544. https://doi.org/10.1002/hep.27141.

Loiola, R.A., Wickstead, E.S., Solito, E., McArthur, S., 2019. Estrogen promotes pro-resolving microglial behavior and phagocytic cell clearance through the actions of annexin A1. Front. Endocrinol. 10 https://doi.org/10.3389/fendo.2019.00420.

Maggioli, E., McArthur, S., Mauro, C., Kieswich, J., Kusters, D.H.M., Reutelingsperger, C. P.M., Yaqoob, M., Solito, E., 2016. Estrogen protects the blood-brain barrier from inflammation-induced disruption and increased lymphocyte trafficking. Brain, Behav.,Immun. 51, 212–222. https://doi.org/10.1016/j.bbi.2015.08.020.

McArthur, S., Cristante, E., Paterno, M., Christian, H., Roncaroli, F., Gillies, G., Solito, E., 2010. Annexin A1: a central player in the anti-inflammatory and neuroprotective role of microglia. J. Immunol. 185, 6317–6328. https://doi.org/10.4049/jimmunol.1001095. Baltimore, Md. : 1950.

McArthur, S., Loiola, R.A., Maggioli, E., Errede, M., Virgintino, D., Solito, E., 2016. The restorative role of annexin A1 at the blood-brain barrier. Fluids Barriers CNS 13, 17. https://doi.org/10.1186/s12987-016-0043-0, 17.

McArthur, S., Juban, G., Gobbetti, T., Desgeorges, T., Theret, M., Gondin, J., Toller-Kawahisa, J.E., Reutelingsperger, C.P., Chazaud, B., Perretti, M., et al., 2020. Annexin A1 drives macrophage skewing to accelerate muscle regeneration through AMPK activation. J. Clin. Invest. 130, 1156–1167. https://doi.org/10.1172/JCI124635.

Mestan, K., Yu, Y., Thorsen, P., Skogstrand, K., Matoba, N., Liu, X., Kumar, R., Hougaard, D.M., Gupta, M., Pearson, C., et al., 2009. Cord blood biomarkers of the fetal inflammatory response. J. Mater. Fetal Neonatal Med: Off. J. Eur. Assoc. Perinatal Med. 22, 379–387. https://doi.org/10.1080/14767050802609759 the Federation of Asia and Oceania Perinatal Societies, the International Society of Perinatal Obstet.

Moretti, R., Pansiot, J., Bettati, D., Strazielle, N., Ghersi-Egea, J.F., Damante, G., Fleiss, B., Titomanlio, L., Gressens, P., 2015. Blood-brain barrier dysfunction in disorders of the developing brain. Front Neurosci 9, 40. https://doi.org/10.3389/fnins.2015.00040.

Mottahedin, A., Smith, P.L., Hagberg, H., Ek, C.J., Mallard, C., 2017. TLR2-mediated leukocyte trafficking to the developing brain. J. Leukocyte Biol. 101, 297–305. https://doi.org/10.1189/jlb.3A1215-568R.

Mottahedin, A., Joakim Ek, C., Truvé, K., Hagberg, H., Mallard, C., 2019. Choroid plexus transcriptome and ultrastructure analysis reveals a TLR2-specific chemotaxis signature and cytoskeleton remodeling in leukocyte trafficking. Brain, Behav. Immun. 79, 216–227. https://doi.org/10.1016/j.bbi.2019.02.004.

Németh, K., Leelahavanichkul, A., Yuen, P.S.T., Mayer, B., Parmelee, A., Doi, K., Robey, P.G., Leelahavanichkul, K., Koller, B.H., Brown, J.M., et al., 2009. Bone marrow stromal cells attenuate sepsis via prostaglandin E2–dependent reprogramming of host macrophages to increase their interleukin-10 production. Nat. Med. 15, 42–49. https://doi.org/10.1038/nm.1905.

Nair, S., Rocha-Ferreira, E., Fleiss, B., Nijboer, C.H., Gressens, P., Mallard, C., Hagberg, H., 2020. Neuroprotection offered by mesenchymal stem cells in perinatal brain injury: role of mitochondria, inflammation, and reactive oxygen species. J. Neurochem. https://doi.org/10.1111/jnc.15267.

Nikiforou, M., Vanderlocht, J., Chougnet, C.A., Jellema, R.K., Ophelders, D.R.M.G., Joosten, M., Kloosterboer, N., Senden-Gijsbers, B.L.M.G., Germeraad, W.T.V., Kramer, B.W., et al., 2015. Prophylactic interleukin-2 treatment prevents fetal gut inflammation and injury in an ovine model of chorioamnionitis. Inflamm. Bowel Dis. 21, 2026–2038. https://doi.org/10.1097/mib.0000000000000455.

Ophelders, D.R.M.G., Gussenhoven, R., Klein, L., Jellema, R.K., Westerlaken, R.J.J., Hütten, M.C., Vermeulen, J., Wassink, G., Gunn, A.J., Wolfs, T.G.A.M., 2020. Preterm brain injury, antenatal triggers, and therapeutics: timing is key. Cells 9, 1871. https://doi.org/10.3390/cells9081871.

Park, J.C., Baik, S.H., Han, S.H., Cho, H.J., Choi, H., Kim, H.J., Choi, H., Lee, W., Kim, D. K., Mook-Jung, I., 2017. Annexin A1 restores Aβ(1-42) -induced blood-brain barrier disruption through the inhibition of RhoA-ROCK signaling pathway. Aging cell 16, 149–161. https://doi.org/10.1111/acel.12530.

Paton, M.C.B., McDonald, C.A., Allison, B.J., Fahey, M.C., Jenkin, G., Miller, S.L., 2017. Perinatal brain injury as a consequence of preterm birth and intrauterine inflammation: designing targeted stem cell therapies. Front. in Neurosci. 11, 200. https://doi.org/10.3389/fnins.2017.00200, 200.

Paton, M.C.B., Allison, B.J., Li, J., Fahey, M.C., Sutherland, A.E., Nitsos, I., Bischof, R.J., Dean, J.M., Moss, T.J.M., Polglase, G.R., et al., 2018. Human umbilical cord blood therapy protects cerebral white matter from systemic LPS exposure in preterm fetal sheep. Dev. Neurosci. 40, 258–270. https://doi.org/10.1159/000490943.

Paton, M.C.B., Allison, B.J., Fahey, M.C., Li, J., Sutherland, A.E., Pham, Y., Nitsos, I., Bischof, R.J., Moss, T.J., Polglase, G.R., et al., 2019. Umbilical cord blood versus mesenchymal stem cells for inflammation-induced preterm brain injury in fetal sheep. Pediatric Res. 86, 165–173. https://doi.org/10.1038/s41390-019-0366-z.

Perretti, M., D'Acquisto, F., 2009. Annexin A1 and glucocorticoids as effectors of the resolution of inflammation. Nat.Rev. Immunol. 9, 62–70. https://doi.org/10.1038/nri2470.

Prame Kumar, K., Nicholls, A.J., Wong, C.H.Y., 2018. Partners in crime: neutrophils and monocytes/macrophages in inflammation and disease. Cell Tissue Res. 371, 551–565. https://doi.org/10.1007/s00441-017-2753-2.

Prinz, M., Priller, J., 2017. The role of peripheral immune cells in the CNS in steady state and disease. Nature neuroscience 20, 136–144. https://doi.org/10.1038/nn.4475.

Rackham, C.L., Vargas, A.E., Hawkes, R.G., Amisten, S., Persaud, S.J., Austin, A.L., King, A.J., Jones, P.M., 2016. Annexin A1 is a key modulator of mesenchymal stromal cell-mediated improvements in islet function. Diabetes 65, 129–139. https://doi.org/10.2337/db15-0990.

Raffaghello, L., Bianchi, G., Bertolotto, M., Montecucco, F., Busca, A., Dallegri, F., Ottonello, L., Pistoia, V., 2008. Human mesenchymal stem cells inhibit neutrophil apoptosis: a model for neutrophil preservation in the bone marrow niche. Stem Cell. 26, 151–162. https://doi.org/10.1634/stemcells.2007-0416.

Rand, K.M., Austin, N.C., Inder, T.E., Bora, S., Woodward, L.J., 2016. Neonatal infection and later neurodevelopmental risk in the very preterm infant. J. Pediatric. 170, 97–104. https://doi.org/10.1016/j.jpeds.2015.11.017.

Ravanidis, S., Bogie, J.F.J., Donders, R., Deans, R., Hendriks, J.J.A., Stinissen, P., Pinxteren, J., Mays, R.W., Hellings, N., 2017. Crosstalk with inflammatory macrophages shapes the regulatory properties of multipotent adult progenitor cells. Stem Cell. Int. 2017, 2353240. https://doi.org/10.1155/2017/2353240.

Rayasam, A., Faustino, J., Lecuyer, M., Vexler, Z.S., 2020. Neonatal stroke and TLR1/2 ligand recruit myeloid cells through the choroid plexus in a CX3CR1-CCR2- and context-specific manner. J. Neurosci. 40, 3849–3861. https://doi.org/10.1523/JNEUROSCI.2149-19.2020.

Ries, M., Loiola, R., Shah, U.N., Gentleman, S.M., Solito, E., Sastre, M., 2016. The anti-inflammatory Annexin A1 induces the clearance and degradation of the amyloid-beta peptide. J. Neuroinflammation 13, 234. https://doi.org/10.1186/s12974-016-0692-6.

Romero, R., Savasan, Z.A., Chaiworapongsa, T., Berry, S.M., Kusanovic, J.P., Hassan, S. S., Yoon, B.H., Edwin, S., Mazor, M., 2011. Hematologic profile of the fetus with systemic inflammatory response syndrome. J. perinatal Med. 40, 19–32. https://doi.org/10.1515/jpm.2011.100.

Sabic, D., Koenig, J.M., 2020. A perfect storm: fetal inflammation and the developing immune system. Pediatric. Res. 87, 319–326. https://doi.org/10.1038/s41390-019-0582-6.

Sato, Y., Ochiai, D., Abe, Y., Masuda, H., Fukutake, M., Ikenoue, S., Kasuga, Y., Shimoda, M., Kanai, Y., Tanaka, M., 2020. Prophylactic therapy with human amniotic fluid stem cells improved survival in a rat model of lipopolysaccharide-induced neonatal sepsis through immunomodulation via aggregates with peritoneal macrophages. Stem cell Res. Ther. 11, 300. https://doi.org/10.1186/s13287-020-01809-1.

Saunders, N.R., Dziegielewska, K.M., Møllgård, K., Habgood, M.D., 2019. Recent developments in understanding barrier mechanisms in the developing brain: drugs and drug transporters in pregnancy, susceptibility or protection in the fetal brain? Ann. Rev. Pharmacol. Toxicol. 59, 487–505. https://doi.org/10.1146/annurev-pharmtox-010818-021430.

Schwartz, M., Baruch, K., 2014. The resolution of neuroinflammation in neurodegeneration: leukocyte recruitment via the choroid plexus. EMBO J. 33, 7–22. https://doi.org/10.1002/embj.201386609.

Shechter, R., London, A., Schwartz, M., 2013a. Orchestrated leukocyte recruitment to immune-privileged sites: absolute barriers versus educational gates. Nat. Rev. Immunol. 13, 206–218. https://doi.org/10.1038/nri3391.

Shechter, R., Miller, O., Yovel, G., Rosenzweig, N., London, A., Ruckh, J., Kim, K.W., Klein, E., Kalchenko, V., Bendel, P., et al., 2013b. Recruitment of beneficial M2 macrophages to injured spinal cord is orchestrated by remote brain choroid plexus. Immunity 38, 555–569. https://doi.org/10.1016/j.immuni.2013.02.012.

Smyth, L.C., Rustenhoven, J., Park, T.I.-H., Schweder, P., Jansson, D., Heppner, P.A., O'Carroll, S.J., Mee, E.W., Faull, R.L., Curtis, M., 2018. Unique and shared inflammatory profiles of human brain endothelia and pericytes. J. Neuroinflammation 15, 1–18.

Stolp, H.B., Dziegielewska, K.M., Ek, C.J., Habgood, M.D., Lane, M.A., Potter, A.M., Saunders, N.R., 2005. Breakdown of the blood–brain barrier to proteins in white matter of the developing brain following systemic inflammation. Cell Tissue Res. 320, 369–378. https://doi.org/10.1007/s00441-005-1088-6.

Sugimoto, M.A., Vago, J.P., Teixeira, M.M., Sousa, L.P., 2016. Annexin A1 and the resolution of inflammation: modulation of neutrophil recruitment, apoptosis, and clearance, 2016 J Immunol Res 8239258. https://doi.org/10.1155/2016/8239258, 8239258.

Szmydynger-Chodobska, J., Strazielle, N., Zink, B.J., Ghersi-Egea, J.-F., Chodobski, A., 2009. The role of the choroid plexus in neutrophil invasion after traumatic brain

injury. J. Cerebral Blood Flow Metab. 29, 1503–1516. https://doi.org/10.1038/jcbfm.2009.71.
Szmydynger-Chodobska, J., Strazielle, N., Gandy, J.R., Keefe, T.H., Zink, B.J., Ghersi-Egea, J.-F., Chodobski, A., 2012. Posttraumatic invasion of monocytes across the blood-cerebrospinal fluid barrier. J. Cereb. Blood Flow Metab. 32, 93–104. https://doi.org/10.1038/jcbfm.2011.111.
Tovar, I., Guerrero, R., López-Peñalver, J.J., Expósito, J., Ruiz de Almodóvar, J.M., 2020. Rationale for the use of radiation-activated mesenchymal stromal/stem cells in acute respiratory distress syndrome. Cells 9. https://doi.org/10.3390/cells9092015.
Uccelli, A., Moretta, L., Pistoia, V., 2008. Mesenchymal stem cells in health and disease. Nature Reviews Immunology 8, 726–736.
Vaes, J.E.G., Vink, M.A., de Theije, C.G.M., Hoebeek, F.E., Benders, M.J.N.L., Nijboer, C. H.A., 2019. The potential of stem cell therapy to repair white matter injury in preterm infants: lessons learned from experimental models. Fronti. Physiol. 10 https://doi.org/10.3389/fphys.2019.00540.
van Well, G.T.J., Daalderop, L.A., Wolfs, T., Kramer, B.W., 2017. Human perinatal immunity in physiological conditions and during infection. Mol. Cell. Pediatric. 4, 4. https://doi.org/10.1186/s40348-017-0070-1.
Walker, P.A., Shah, S.K., Jimenez, F., Gerber, M.H., Xue, H., Cutrone, R., Hamilton, J.A., Mays, R.W., Deans, R., Pati, S., 2010. Intravenous multipotent adult progenitor cell therapy for traumatic brain injury: preserving the blood brain barrier via an interaction with splenocytes. Exp. Neurol. 225, 341–352.
Walker, P.A., Bedi, S.S., Shah, S.K., Jimenez, F., Xue, H., Hamilton, J.A., Smith, P., Thomas, C.P., Mays, R.W., Pati, S., 2012. Intravenous multipotent adult progenitor cell therapy after traumatic brain injury: modulation of the resident microglia population. J. Neuroinflammation 9, 228.
Wu, Y.W., Colford Jr., J.M., 2000. Chorioamnionitis as a risk factor for cerebral palsy: a meta-analysis. Jama 284, 1417–1424.
Yan, E., Castillo-Melendez, M., Nicholls, T., Hirst, J., Walker, D., 2004. Cerebrovascular responses in the fetal sheep brain to low-dose endotoxin. Pediatr. Res. 55, 855–863. https://doi.org/10.1203/01.Pdr.0000115681.95957.D4.
Yap, V., Perlman, J.M., 2020. Mechanisms of brain injury in newborn infants associated with the fetal inflammatory response syndrome. In: Proceedings of the Seminars in Fetal and Neonatal Medicine, p. 101110.
Yawno, T., Schuilwerve, J., Moss, T.J., Vosdoganes, P., Westover, A.J., Afandi, E., Jenkin, G., Wallace, E.M., Miller, S.L., 2013. Human amnion epithelial cells reduce fetal brain injury in response to intrauterine inflammation. Dev. Neurosci. 35, 272–282. https://doi.org/10.1159/000346683.
Yawno, T., Sabaretnam, T., Li, J., McDonald, C., Lim, R., Jenkin, G., Wallace, E.M., Miller, S.L., 2017. Human amnion epithelial cells protect against white matter brain injury after repeated endotoxin exposure in the preterm ovine fetus. Cell Transpl. 26, 541–553. https://doi.org/10.3727/096368916X693572.
Yellowhair, T.R., Noor, S., Mares, B., Jose, C., Newville, J.C., Maxwell, J.R., Northington, F.J., Milligan, E.D., Robinson, S., Jantzie, L.L., 2019. Chorioamnionitis in rats precipitates extended postnatal inflammatory lymphocyte hyperreactivity. Dev. Neurosci. 1–11. https://doi.org/10.1159/000497273.
Zagoura, D., Trohatou, O., Makridakis, M., Kollia, A., Kokla, N., Mokou, M., Psaraki, A., Eliopoulos, A.G., Vlahou, A., Roubelakis, M.G., 2019. Functional secretome analysis reveals Annexin-A1 as important paracrine factor derived from fetal mesenchymal stem cells in hepatic regeneration. EBioMedicine 45, 542–552.